Eur. J. Biochem. *150*, 371 – 386 (1985)

Regulation of the human-erythrocyte hexose-monophosphate shunt under conditions of oxidative stress

A study using NMR spectroscopy, a kinetic isotope effect, a reconstituted system and computer simulation

David R. THORBURN and Philip W. KUCHEL

Department of Biochemistry, University of Sydney

(Received December 27, 1984/April 9, 1985) – EJB 84 1341

The regulation of the hexose monophosphate shunt of human erythrocytes under conditions of oxidative stress has been investigated by monitoring the reduction of oxidised glutathione (GSSG) to reduced glutathione (GSH) in erythrocytes containing high levels of GSSG; ^{1}H NMR and a biochemical assay were used to measure the changes.

A reconstituted metabolic system prepared with the purified erythrocyte enzymes was used in conjunction with studies of intact cells and haemolysates to determine the dependence of the rate of GSH production on the activities of hexokinase and glucose-6-phosphate dehydrogenase. Both of these enzymes have previously been claimed to be the rate-limiting step of oxidatively stimulated flux through the hexose monophosphate shunt.

The absence of a kinetic isotope effect on the rate of GSH production in these systems, when [1-^{2}H]glucose replaced glucose as the source of reducing equivalents, showed that glucose-6-phosphate dehydrogenase activity was not a strong determinant of the flux. The dependence of the rate of GSH production on the concentration of the hexokinase inhibitors glucose 1,6-bisphosphate and glycerate 2,3-bisphosphate showed that, under conditions of oxidative stress, hexokinase was the principal determinant of flux through the shunt. Glucose 1,6-bisphosphate at the concentration present *in vivo* appears to be more important in limiting hexokinase activity, and thus the rate of glucose utilisation, than was previously assumed.

A detailed computer model of the system was developed based on the reported kinetic parameters of the enzymes involved. A sensitivity analysis of this model predicted that the hexokinase reaction would have a sensitivity coefficient of 0.995 with respect to the maximal rate of GSH production.

The hexose monophosphate shunt (HMS) provides reducing equivalents in the form of NADPH and pentose sugars for nucleotide metabolism. In human erythrocytes, flux through the HMS maintains glutathione in the reduced form as one of the main cellular anti-oxidative mechanisms [1]. Red cells are regularly subjected to high oxygen tension and are among the first body cells exposed to exogenous oxidative substances that are ingested, injected or inhaled. The importance of this anti-oxidative function is shown by the massive oxidant-induced haemolysis seen in subjects with a marked deficiency of glucose-6-phosphate dehydrogenase (G6PD), the first enzyme unique to the HMS [1].

The regulation of the erythrocyte HMS under oxidatively stressed or unstressed conditions has been extensively studied. In unstressed conditions, 5 – 10% of the total glucose consumption of 1 – 2 mmol h^{-1} (l cell)$^{-1}$ at 37 °C passes through the HMS [2 – 5] and the flux is limited mainly by the G6PD reaction which operates at less than 1% of its capacity; this is largely due to inhibition by the high cellular NADPH:$NADP^+$ ratio of at least 40:1 [6 – 8]. When red cells are subjected to oxidative stress, for example by oxidation of GSH or addition of 0.1 – 0.5 mM methylene blue, 80 – 100% of the total glucose consumed, 2 – 4 mmol h^{-1} (l cell)$^{-1}$, passes through the HMS [2 – 4, 9]. It has been variously suggested that under such conditions the HMS flux is (a) limited by hexokinase (HK) [2, 4], (b) limited by G6PD [3], (c) not limited by HK [5], (d) not limited by G6PD [4, 6] and (e) not limited by GSSG reductase [10, 11].

In this study the regulation of the erythrocyte HMS has been investigated by studying the kinetics of GSH production in red cells containing high levels of GSSG. The enzymes involved in the redox metabolism of GSH are shown in Fig. 1. Rose [6] showed the existence of a hydrogen kinetic isotope effect on G6PD, of magnitude 1.4 – 2.4, with the substrate [1-^{2}H]glucose-6-*P* and we have used this phenomenon to probe the *in situ* regulation of the enzyme. ^{1}H NMR spectroscopy was used for continuous measurement of GSH production in suspensions of human erythrocytes.

The erythrocyte enzymes involved in the maintenance of GSH were purified and used to reconstitute a metabolic system. Enzyme reconstitution has been used previously to identify the *in situ* control principles of metabolic pathways,

Correspondence to P. W. Kuchel, Department of Biochemistry, University of Sydney, Sydney, New South Wales, Australia 2006

Abbreviations. Gluconate-6-*P*, gluconate 6-phosphate; gluconolactone-6-*P*, gluconolactone 6-phosphate; glucose-1,6-P_2, glucose 1,6-bisphosphate; glucose-6-*P*, glucose 6-phosphate; glycerate-2,3-P_2, glycerate 2,3-bisphosphate; G6PD, glucose-6-phosphate dehydrogenase; GSH, reduced glutathione; GSSG, oxidised glutathione; HK, hexokinase; HMS, hexose monophosphate shunt; ribulose-5-*P*, ribulose 5-phosphate.

Enzymes. Gluconate-6-phosphate dehydrogenase (EC 1.1.1.44); glucose-6-phosphate dehydrogenase (EC 1.1.1.49); glutathione peroxidase (EC 1.11.1.9); glutathione reductase (EC 1.6.4.2); hexokinase (EC 2.7.1.1); NAD(P) glycohydrolase (EC 3.2.2.6); 6-phosphogluconolactonase (EC 3.1.1.31).

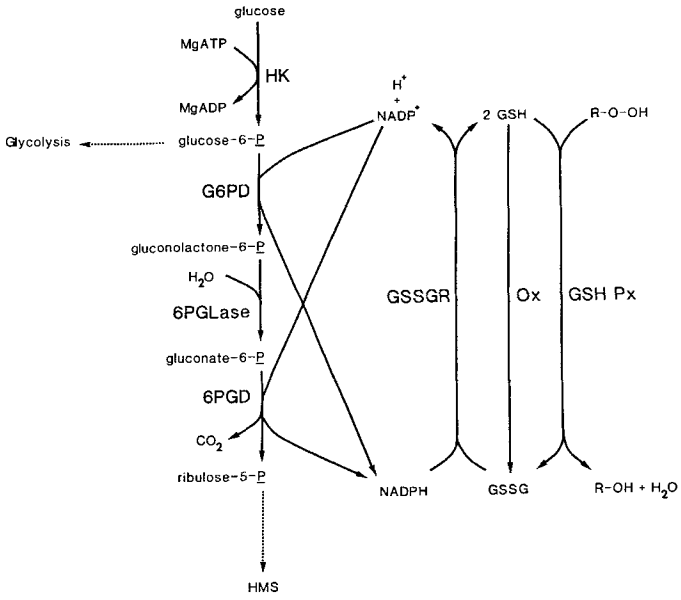

Fig. 1. *Scheme for redox metabolism of GSH of the human erythrocyte.* The scheme consists of the following enzyme-catalysed reactions: HK, hexokinase; G6PD, glucose-6-*P* dehydrogenase; 6PGLase, 6-phosphogluconolactonase; 6PGD, gluconate-6-*P* dehydrogenase; GSSGR, glutathione reductase; GSH Px, glutathione peroxidase; and Ox, other enzymic processes and spontaneous oxidation of GSH. R is $(CH_3)_3C$ for *t*-butyl hydroperoxide

particularly glycolysis [12, 13]. Many investigators have used extensively purified enzymes, often from a variety of different species and/or gel-entrapped enzymes, to reconstitute their metabolic system; our approach was to use semi-purified, well-characterised preparations of human erythrocyte enzymes in free solution. The possibility of artefactual observations, arising from differences in the kinetic characteristics of enzymes from different sources or from enzyme modification during rigorous preparative procedures, should therefore have been minimised.

Computer simulation involving sensitivity analysis [14, 15] has allowed a quantitative definition of the contribution of each reaction to the overall flux of reducing equivalents to GSSG. Previous models of the HMS [16, 17] have used simplified flux equations for the individual enzymes to gain a qualitative description of the whole system. In contrast we have attempted to predict the behaviour of the system by using enzyme models based on the known steady-state kinetics of the individual enzymes. This is the only approach that can determine whether the known *in vitro* kinetic data is adequate to explain the observed *in situ* system behaviour.

MATERIALS AND METHODS

Materials

6-Amino-*n*-hexanoic acid, bovine serum albumin (type V), digitonin, 5,5′-dithiobis-(2-nitrobenzoic acid), glucose-6-*P*, glycerate-2,3-P_2, Hepes, $NADP^+$, NADPH, sponin, yeast G6PD and yeast gluconate-6-*P* dehydrogenase were obtained from Sigma Chemical Co. (St Louis, MO, USA). ATP, FAD, gluconate-6-*P*, glucose-1,6-P_2, GSH and GSSG were from Boehringer Mannheim (North Ryde, N.S.W., Australia). Niacinamide was purchased from Calbiochem (Los Angeles, CA, USA), [1-^{2}H]glucose and sodium 2,2-dimethyl-2-silapentane 5-sulfonate were from Merck, Sharp and Dohme (Point Claire-Dorval, Que., Canada) and *t*-butyl hydroperoxide was from Merck (Darmstadt, FRG). The ultrafiltration membranes (types PM10 and PM30) were from Amicon (Lexington, MA, USA). 2′,5′-ADP-Sepharose 4B (adenosine 2′,5′-bisphosphate linked to Sepharose via a 6-aminohexyl group) and DEAE-Sephadex A-50 gels and Sephadex G-25 PD10 columns were from Pharmacia (Uppsala, Sweden). Carbogen was from Commonwealth Industrial Gases (Alexandria, N.S.W., Australia). All other reagents were of A. R. grade.

Cell preparation

Glucose-free human erythrocytes were prepared from freshly drawn venous blood by washing twice in isotonic saline and twice in Krebs bicarbonate buffer containing antibiotics [18]; the supernatant solution and buffy coat were removed by aspiration. The haematocrit of samples was adjusted to 0.8 for ^{1}H NMR experiments or 0.5–0.6 for other experiments. Haemolysates were prepared by sonication (2×10 s, 40 W output, Branson sonifier model B-12) of the cell suspensions (haematocrit > 0.9) with 25 mM niacinamide [19].

Time courses of GSSG reduction

Cellular GSH was quantitatively oxidised using *t*-butyl hydroperoxide [20]; it was necessary to make the peroxide equimolar with GSH to oxidise the GSH completely. Incubations of cells or haemolysates were carried out in sealed 25-ml conical flasks with shaking at 37°C and with an humidified stream of Carbogen (O_2:CO_2 = 19:1). GSH was determined at specified times using the 5,5′-dithiobis-(2-nitrobenzoic acid) method [21] adapted to a centrifugal analyser (Centrifichem 300, Union Carbide Corp., Tarrytown, NY, USA). Concentrations were expressed per litre of cell water, assuming 0.7 l cell water (l packed cells)$^{-1}$ [21].

NMR studies were carried out in a Bruker WM400 spectrometer at 400 MHz for ^{1}H in the pulsed Fourier mode. Pre-treatment of samples and spectral-acquisition parameters were as described elsewhere [19]. The relative redox status of GSH was determined from the ratio of the amplitudes of the GSH-glutamyl H4 and H3 resonances; the amplitude of the latter resonance was independent of the GSH:GSSG ratio.

All cell and haemolysate experiments mentioned here were carried out with blood from a single donor (DRT); this was done in order to minimise biological variation. The donor was a healthy male Caucasian with normal levels of the enzymes and metabolites studied (Table 1). The normal time course of GSH production in cells from this donor was essentially complete in about 25 min; this agrees with other reports [20] and with time courses from other donors (data not presented here).

Enzyme assays

The activities of HK, G6PD, gluconate-6-*P* dehydrogenase and GSSG reductase were determined in simulated physiological conditions at 37°C (50 mM Hepes, pH 7.20 at 37°C, I = 0.15 M) using the centrifugal analyser. The HK assay mixture also contained 85 mM KCl, 10 mM $MgCl_2$, 5 mM ATP, 1 mM EDTA, 0.5 mM $NADP^+$, 5 mM glucose, 0.1 U ml^{-1} G6PD and 0.1 U ml^{-1} gluconate-6-*P* dehydrogenase [concentrations refer to the final (cuvette) concentrations

Table 1. *Levels of enzymes, haemoglobin and metabolites in erythrocytes*
The haemoglobin concentration and activities of some enzymes in red blood cells from 12 healthy donors are presented. The enzyme assays were done at pH 7.2, $I = 0.15$ M, 37°C; haemoglobin was determined by the cyanmethaemoglobin method [22] adapted to the centrifugal analyser. Values are also presented for cells from the donor whose blood was used in all time course experiments. The levels of some metabolites in the blood of the donor and the normal levels determined by Beutler [21] are also given. The metabolite assays were adapted to the centrifugal analyser from the procedures of Beutler [21] (ATP and GSH) and Hickey et al. [23] (glycerate-2,3-P_2). All estimates of parameters in multiple donors are given as mean ± standard deviation. The coefficient of variation of individual estimates was < 5% for all assays except HK activity where it was about 10%

Component	Amount in	
	normal controls	single donor
	μmol min^{-1} (l cell water)$^{-1}$	
HK	260 ± 40	243
G6PD	3870 ± 230	3750
Gluconate-6-*P* dehydrogenase	4490 ± 300	4240
GSSG reductase	2940 ± 530	2840
Haemoglobin	g (l cell)$^{-1}$	
	329 ± 15	320
	mmol (l cell water)$^{-1}$	
GSH	3.2 ± 0.5	2.72 ± 0.26[a]
ATP	2.05 ± 0.14	1.9
Glycerate-2,3-P_2	6.0 ± 0.9	7.1

[a] Mean ± standard deviation of 11 estimates taken over a 2-year period.

of the reagents]. The change in absorbance at 340 nm was calculated over six 4-min intervals, commencing 10 min after mixing. The sample volume was 32 μl (1/20 diluted lysate) in a final (cuvette) volume of 432 μl. The amount of enzyme which catalysed the reduction of 2 μmol $NADP^+$ min^{-1} under these conditions was defined as 1 U of HK activity.

The gluconate-6-*P* dehydrogenase assay mixture contained 50 mM Hepes, 105 mM KCl, 5 mM $MgCl_2$, 1 mM EDTA, 0.5 mM $NADP^+$ and 1 mM gluconate-6-*P*. The change in absorbance at 340 nm was calculated over four 1-min intervals, commencing 3 min after mixing and the sample volume was 20 μl (1/24 diluted lysate) in a final volume of 420 μl. G6PD activity was determined in the same way except that 1 mM gluconate-6-*P* was replaced by 1 mM glucose-6-*P*. The reagent also contained 0.1 U ml^{-1} gluconate-6-*P* dehydrogenase and readings were not commenced until 8 min after mixing. Haemolysates for these two assays were prepared by addition of 1 vol. cells to 5 vol. of an aqueous solution of 0.2% (w/v) digitonin, 15 μM $NADP^+$; complete lysis was achieved in 10 min at room temperature. The amount of enzyme which catalysed the reduction of 1 (2) μmol $NADP^+$ min^{-1} under these conditions was defined as 1 U of gluconate-6-*P* dehydrogenase (G6PD) activity.

The GSSG reductase assay mixture contained 50 mM Hepes, 110 mM KCl, 5 mM $MgCl_2$, 1 mM EDTA, 1 mM GSSG and 0.1 mM NADPH (spectrophotometrically standardised). The change in absorbance at 340 nm (referenced to H_2O with correction for oxidation in the absence of sample) was calculated over six 1-min intervals, commencing 4 min after mixing and the sample volume was 20 μl (1/60 diluted lysate) in a final volume of 420 μl. Cell samples were diluted in stabilising solution [21] and sonicated (1 × 10 s, 40 W output) prior to assay. The amount of enzyme which catalysed the oxidation of 1 μmol NADPH min^{-1} under these conditions was defined as 1 U of GSSG reductase activity.

Appropriate dilutions (in stabilising solution plus 1 mg ml^{-1} bovine serum albumin) of the purified erythrocyte enzymes were assayed in the same way.

Reconstitution experiments

The procedures used in the enzyme purifications are given in detail in the Supplement at the end of the paper. The reconstituted metabolic systems were prepared in 50 mM Hepes buffer (pH 7.20 at 37°C) and were incubated at 37°C. The total volume was 1.0 ml and typically contained 0.052 U HK, 0.774 U G6PD, 0.898 U gluconate-6-*P* dehydrogenase, 0.588 U GSSG reductase, 0.1 mg bovine serum albumin, 1.43 μmol GSSG, 65 nmol $NADP^+$, 5 μmol $MgCl_2$, 10 μmol glucose, 0.3 μmol EDTA, 2.5 μmol ATP and KCl to give an ionic strength of 0.15 M. All constituents except the ATP were added to the tubes; these were incubated for 5 min prior to the addition of ATP. Samples (40 μl) were then periodically removed for GSH estimation. The activities of all the enzyme preparations were assayed within 24 h prior to commencing an experiment. The contamination of each preparation with the other enzymes was determined and allowed for in calculating the volumes needed to achieve the desired final activity of each enzyme: a computer program which solves simultaneous algebraic equations by matrix inversion was written in BASIC and used to determine the necessary volumes of each preparation.

The enzyme activities were chosen to correspond to one fifth the 'normal' assayed levels (Table 1) and the GSSG concentration was half the 'normal' GSH level measured in cells from the donor used in time course experiments. Since the NADP of glucose-free cells treated with *t*-butyl hydroperoxide would be, essentially, all in the oxidised form, the $NADP^+$ concentration used corresponds to the reported (total) NADP level [7]. The initial MgATP concentration was higher than the calculated intracellular level of 1.44 mmol (l cell water)$^{-1}$ [24] to ensure that an adequate level was maintained throughout the time course.

Numerical methods

The computer-simulation model of GSSG reduction was based on the published kinetic mechanisms of each of the enzymes involved. The rate equation for each mechanism was derived and from this the relations between the steady-state kinetic parameters and the unitary rate constants were determined. These relations were incorporated into a series of computer programs written in BASIC which were used to change iteratively the values of the rate constants until a set was obtained which was consistent with the published values of the steady-state kinetic parameters for that enzyme. The range through which the rate constants were varied was constrained by consideration of diffusion limitation of enzyme-catalysed reactions ($k < \approx 10^9$ M^{-1} s^{-1}) [25]. The kinetic behaviour of each enzyme model was verified by simulations used to construct the appropriate Lineweaver-

Burk and Dixon plots which, in all cases, predicted the expected values of the steady-state kinetic parameters. The details of the computer-simulation model are given in the Supplement.

The reaction mechanisms and the values of rate constants and concentrations define the simulation scheme. The BIOSSIM package [26] (obtained from the SHARE program library agency, Triangle Universities Computation Centre, NC, USA) was used to perform the simulations on a Cyber 720 computer. A simulation scheme was also derived which calculates the concentrations of Mg^{2+}-bound, HbO_2-bound or free glycerate-2,3-P_2 and ATP based on the reported association constants for simulated intracellular conditions [27]. Alternatively, the program of Perrin and Sayce [28] was used to calculate the concentrations of free and bound metals and ligands.

The initial rates of GSH production (v_{GSH}) or of increase of relative peak amplitude (NMR time courses) were estimated by regression of a line onto the initial part of the time course. This analysis routinely gave a lower error in the parameters and a smaller sum of the residuals than regressing a non-linear expression onto all, or part, of the time course. The non-linear fits tended to show a systematic deviation from the time course data. The observed kinetic isotope effect (k_H/k_D) was the ratio of the initial rate with glucose as substrate compared to that with [1-^{2}H]glucose as substrate.

The weighted mean of repeated estimates was calculated using the reciprocal of the squared standard deviation as the weighting factor. The grouped standard deviation ($\bar{\sigma}$) of this estimate was calculated using the following equation:

$$\bar{\sigma} = \sqrt{\left(1/\sum_{i=1}^{n} 1/\sigma_i^2\right)}.$$

A sensitivity analysis [14, 15] of the computer-simulation model was performed by varying the value of the concentration of each enzyme, one at a time, through 12 or more concentrations in the range 0.1−200% of the value in the normal system. The plot of maximal flux of GSH in the simulation versus enzyme concentration, relative to their normal values, gave the 'sensitivity profile' of that component with respect to the overall system. A quadratic function was then fitted to the data near the normal 'system' concentration of the component using least-squares regression analysis. The sensitivity coefficient for the component was defined as the value of the first derivative of the function at the normal system value. The sensitivity coefficient of the hydrolysis step of 6-phosphogluconolactone was calculated by varying the enzyme concentration and the rate constant for spontaneous hydrolysis simultaneously through the range 0.1−200% of normal in the same way.

BASIC programs were run on a Tektronix 4052 graphics computer. Non-linear regression analysis was performed as described elsewhere [19].

RESULTS

GSSG reduction in intact cell preparations

Fig. 2 shows a series of ^{1}H-NMR spin-echo spectra obtained from a suspension of intact erythrocytes initially treated with *t*-butyl hydroperoxide and then incubated with 10 mM glucose. The amplitude of the GSH-glutamyl H3 resonance did not change significantly during GSSG reduction. When referenced to another unchanging resonance, ergothioneine-$N^+(CH_3)_3$, the coefficient of variation of the mean GSH-glutamyl H3/ergothioneine ratio was typically about 6%; regression of a line onto the data yielded a slope that was typically about 0.2 ± 0.1% of the mean value (units min^{-1}) which was considered to be negligible over the period of study. However, the amplitude of the GSH-glutamyl H4 resonance increased markedly and we were thus able to construct time courses of relative GSH increase (Fig. 3A). Similar time courses were obtained by using the chemical assay for GSH (Fig. 3B).

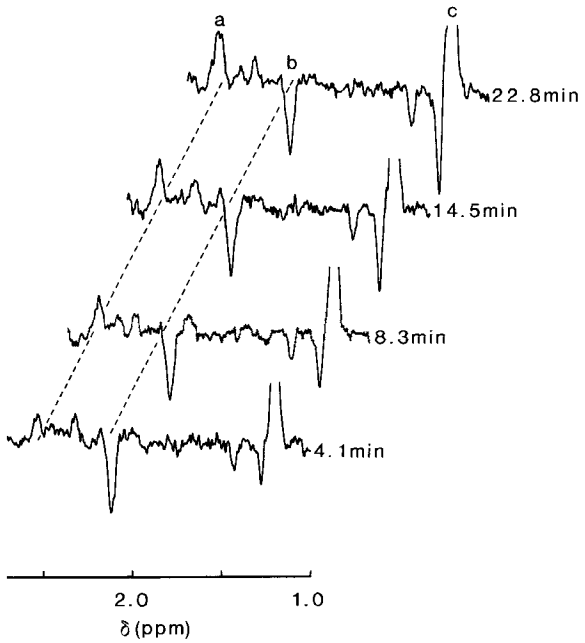

Fig. 2. *400-MHz ^{1}H-NMR spin-echo spectra of a suspension of intact human erythrocytes (haematocrit = 0.86) to which* t-*butyl hydroperoxide (10 µl of a 0.08 M solution) was added at −5 min and glucose (10 µl of a 0.5 M solution) at 0 min.* Each spectrum consisted of 64 transients digitised into 8 k points with a spectral width of 5 kHz; a 1.0-s homogated water saturation pulse was used and the total accumulation time was 124 s. Chemical shift (δ) is shown relative to sodium 2,2-dimethyl-2-silapentane 5-sulfonate (δ = 0.000 ppm). Spectral assignments: a, GSH-glutamyl H4; b, GSH-glutamyl H3; c, *t*-butanol methyl protons

No significant kinetic isotope effect on v_{GSH} was detected using the two assay methods with intact erythrocytes (Table 2). Despite using cells from only one donor, individual estimates of v_{GSH} over a period of 2 years differed by up to 20% from the weighted mean value.

When the incubation buffer was that used by Magnani et al. [5], containing 27 mM P_i, the calculated value of v_{GSH} was about 24% higher than for cells incubated in Krebs bicarbonate buffer. However, when the rate was corrected, according to [29], for the smaller cell volume caused by the high osmolality of the P_i buffer, the calculated v_{GSH} was not significantly different from the normal value; also, no significant kinetic isotope effect was found (Table 2).

GSSG reduction in haemolysates

Only slow and incomplete GSH production was seen in haemolysates prepared by freezing and thawing. In haemolysates prepared by sonication, however, the time course of GSH production, following administration of *t*-butyl hydroperoxide and addition of glucose, was comparable to

that in intact cells [v_{GSH} = 9.1 ± 0.3 mmol h^{-1} (l lysate water)$^{-1}$, Table 2]. The differences in GSH production in the two types of lysate correlate with the reported changes in ATP concentration following haemolysis [30]. In lysates prepared by freezing and thawing, in the presence of 10 mM glucose, we found that the ATP level fell by more than 90% in 30 min while in lysates prepared by sonication (with 10 mM glucose) the ATP concentration was maintained at the initial level over this period.

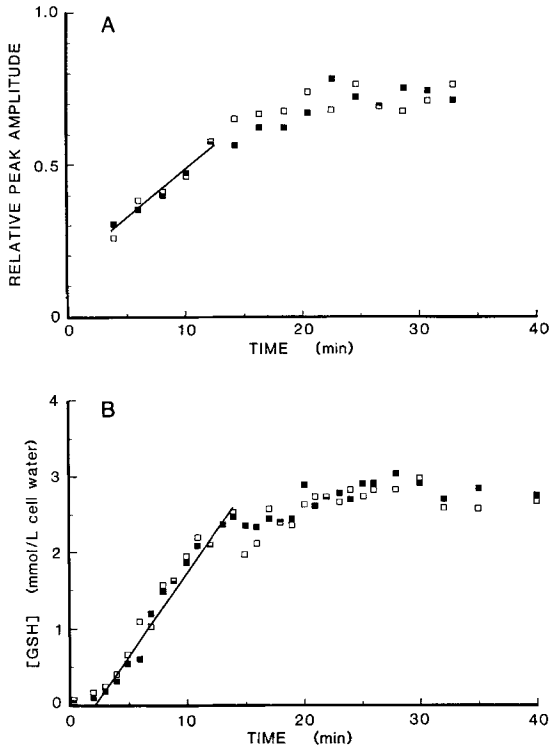

Fig. 3. *Time courses of GSH production in intact erythrocytes measured using (A) ^{1}H-NMR spectroscopy and (B) a chemical assay.* *t*-Butyl hydroperoxide was added to the glucose-free cell suspensions at −5 min at a concentration equimolar with the GSH and the cell suspensions were brought to 37 °C. (■) Glucose or (□) [1-^{2}H]glucose was added to the cell suspensions at 0 min at a final concentration of 10 mM. The solid lines are linear regressions onto the initial part of the glucose data set

In lysates prepared by sonication, a significant isotope effect was detected (Table 2). This means that although v_{GSH} was only slightly lower, G6PD was relatively more rate-limiting following sonication. When $NADP^+$ (1 mM), sufficient to saturate G6PD, was added to the lysate prior to starting the experiment, the value of k_H/k_D fell to a non-significant value and v_{GSH} increased to the value determined in intact cells (Table 2). This suggests that the isotope effect observed in lysates in the absence of added $NADP^+$ was due to a fall in the $NADP^+$ level, possibly as a result of incomplete inhibition of NAD(P) glycohydrolase by the added 25 mM niacinamide. As there was no significant difference in k_H/k_D or in v_{GSH} in lysates (plus $NADP^+$) and intact cells, the lysate (plus $NADP^+$) appears to be a good system for studying the regulation of GSSG reduction for comparison with intact cells.

Addition of the HK inhibitor glucose-1,6-P_2 to the lysate (plus $NADP^+$) caused a significant reduction in v_{GSH} (Table 2); when glucose-1,6-P_2 was added to increase the concentration by 0.1 and 0.2 mmol l^{-1}, v_{GSH} fell to 64.5 ± 2.6% and 43.1 ± 1.9%, respectively, of the value determined in the absence of added glucose-1,6-P_2. The initial level of glucose-1,6-P_2 was not measured but was assumed to be 0.1 mmol l^{-1} lysate water [31].

The HK activity of diluted lysate, prepared from washed erythrocytes, was assayed as described in the Methods except that the ATP concentration was 1.5 mM and various amounts of glucose-1,6-P_2 were added to the assay system. In the presence of 0.2 mM and 0.3 mM glucose-1,6-P_2 the HK activity was 76% and 52%, respectively, of the activity in the presence of 0.1 mM glucose-1,6-P_2. The concentrations of glucose-1,6-P_2 in this comparison are approximately the same as those found in the lysates. We found negligible (< 10%) inhibition of the activities of G6PD, gluconate-6-*P* dehydrogenase and GSSG reductase by 0.3 mM glucose-1,6-P_2 when assayed as described in the Methods, or using the same assays without $MgCl_2$. The higher inhibition of v_{GSH} in the lysate, compared to the effect on HK in the assay medium, by apparently comparable levels of glucose-1,6-P_2 is discussed later.

GSSG reduction in the reconstituted metabolic system

The enzyme activities used in the reconstituted system were set at one fifth the measured red cell values because preliminary computer simulations had predicted that the rate

Table 2. *GSH production in erythrocyte preparations*
The GSH content of intact cells or sonicate lysates was quantitatively oxidised with *t*-butyl hydroperoxide (see Methods). The rate of GSH production (v_{GSH}) was determined using the chemical assay in samples supplied with 10 mM glucose and with or without other metabolites. The kinetic isotope effect (k_H/k_D) was determined in paired samples supplied with glucose or [1-^{2}H]glucose using the chemical assay or ^{1}H NMR method. The number of experiments is given in parentheses and values are given as weighted mean ± grouped standard deviation as described in the Methods

Preparation	v_{GSH}	k_H/k_D
	mmol h^{-1} (l cell water)$^{-1}$	
Intact cells	10.32 ± 0.29 (5)	1.00 ± 0.04 (8)
Intact cells + P_i[a]	10.86 ± 0.27 (1)	1.02 ± 0.03 (1)
Lysate	9.06 ± 0.32 (2)	1.27 ± 0.07 (2)
Lysate + 1 mM $NADP^+$	10.31 ± 0.17 (2)	1.06 ± 0.05 (1)
Lysate + 1 mM $NADP^+$ + 0.1 mM glucose-1,6-P_2	6.65 ± 0.13 (1)	–
Lysate + 1 mM $NADP^+$ + 0.2 mM glucose-1,6-P_2	4.44 ± 0.12 (1)	–

[a] Cells were washed in a medium containing 27 mM P_i, as described by Magnani et al. [5]. The rate estimate was corrected for the higher osmolality of this buffer as described in the Results.

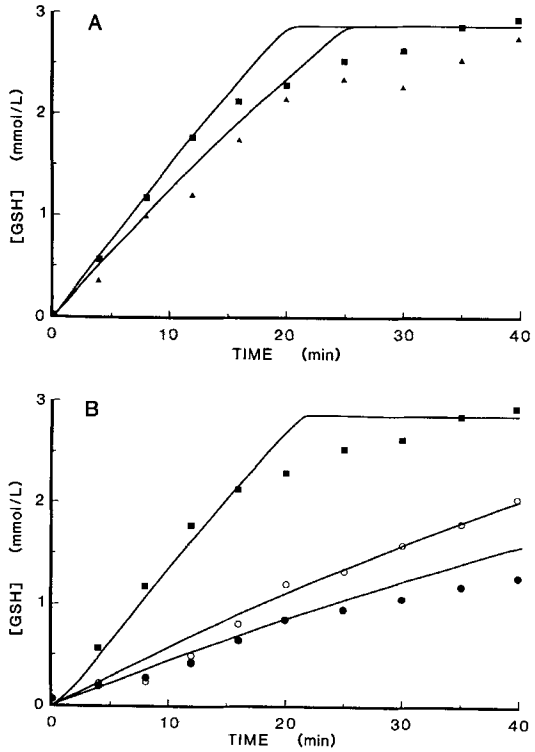

Fig. 4. *Time courses of GSH production in a reconstituted metabolic system in (■) the absence of effectors or in the presence of (A) (▲) 3.2 mM free glycerate-2,3-P_2, (B) (○) 0.2 mM glucose-1,6-P_2 or (●) 0.3 mM glucose-1,6-P_2.* The composition of the reconstituted system is given in Methods. The reaction was started at 0 min by the addition of ATP; GSH concentration was estimated chemically. The solid lines are computer simulations of the corresponding systems. In the simulation of the system with no effectors present in (B) (■) it was assumed that the rate constant for spontaneous hydrolysis of gluconolactone-6-*P* had a value of $7.7 \times 10^{-3}\ s^{-1}$ [34] and that 6-phosphogluconolactonase was absent. In the other simulations shown it was assumed that the rate constant had a value of $7.1 \times 10^{-4}\ s^{-1}$ [33] and that the enzyme activity was 4.80 units ml^{-1}; this activity of 6-phosphogluconolactonase, relative to the other enzymes, was the same as assumed for the intact cell (see Supplement)

Table 3. *GSH production in the reconstituted metabolic system*
The relative rate of glutathione production in reconstituted systems, to which various effectors had been added, is expressed as a percentage of the v_{GSH} (43.7 ± 0.7 mmol $h^{-1}\ l^{-1}$) observed in the basic system. Values are given as mean ± standard deviation of the relative rate estimate; the number of experiments is given in parentheses

Effector(s) added	v_{GSH}
	%
None	100.0 ± 1.6 (2)
1.0 mM P_i	109 ± 4 (1)
0.2 mM glucose-1,6-P_2	34.5 ± 1.3 (1)
0.3 mM glucose-1,6-P_2	21.9 ± 0.8 (1)
0.2 mM glucose-1,6-P_2 + 1 mM P_i	63 ± 5 (1)
3.2 mM free glycerate-2,3-P_2[a]	73 ± 4 (1)
4.91 mM MgATP[a]	112 ± 4 (1)

[a] The concentrations of free and Mg^{2+}-bound effectors were calculated as described in the Methods.

of GSH production, using higher activities, would be too fast to follow experimentally with accuracy. Thus rates of GSH production were expressed per litre cell water by multiplying the measured rate by five. Fig. 4A and 4B show time courses of GSH production in the reconstituted system with addition of the putative effector molecules, glycerate-2,3-P_2 and glucose-1,6-P_2.

In the reconstituted system, with glucose as substrate and without added effector molecules, $v_{GSH} = 43.7 \pm 0.7$ mmol h^{-1} (l cell water)$^{-1}$; this rate was 4.23 ± 0.14 times the value found in intact cells. When [1-^{2}H]glucose replaced glucose, $k_H/k_D = 1.00 \pm 0.09$. If HK activity was an important cellular determinant of v_{GSH} then part of the difference in v_{GSH} in the reconstituted system compared to the intact cell could have been due to the higher initial concentration of MgATP in the former. This was calculated to be 2.41 mM compared to the reported intracellular level of 1.44 mmol (l cell water)$^{-1}$ [24]. Using the initial rate equation for HK [32], and the initial metabolite concentrations used in the reconstituted system, we calculated that the higher concentration of MgATP would increase HK activity by 13.4%. The difference in MgATP concentration can therefore account for only a small proportion of the approximately 400% increase in v_{GSH} in the reconstituted system compared to the intact cell suspension.

The effect of various modifiers of HK activity on the rate of GSH production is summarised in Table 3. v_{GSH} in the reconstituted system was markedly reduced by glucose-1,6-P_2. The degree of inhibition was in fact greater than the inhibition of HK in the assay medium (with 1.5 mM ATP) by the same concentrations of inhibitor; 0.2 mM and 0.3 mM glucose-1,6-P_2 reduced HK activity to 59% and 40%, respectively, of the activity in the absence of inhibitor. The inhibition of v_{GSH} was partly relieved by the physiological concentration of P_i (1 mM). The dependence of v_{GSH} on the concentrations of glycerate-2,3-P_2 and MgATP also mirrored the expected dependence of HK activity on these metabolites.

In another experiment with relatively higher HK activity (based on the levels reported by Beutler [21] for pH 8.0; in 1.0 ml: 0.048 U HK, 0.329 U G6PD, 0.345 U gluconate-6-*P* dehydrogenase, 0.287 U GSSG reductase) we found no significant change in the rate of GSH production when the G6PD activity was decreased by 50% but the rate fell by 40% when the HK activity was halved.

Computer simulation of GSSG reduction

The activity of 6-phosphogluconolactonase was not assayed in the enzyme preparations; the purification of the enzyme from bovine erythrocytes and a suitable enzymic assay have only recently been reported [33]. It was necessary to assume that the enzyme was present at a low level (for example 10% with respect to the other enzymes) or to use a rate constant for spontaneous hydrolysis derived from earlier work [34] in order that the simulated time course agreed with that measured in the reconstituted system.

Computer simulations of some of the reconstituted metabolic systems are shown in Fig. 4. In these simulations the enzymic activities and initial metabolite concentrations were set at the levels used in the experiments. Simulation of a kinetic isotope effect on G6PD (equivalent to using [1-^{2}H]glucose-6-*P* as substrate and invoked by decreasing k_5 and k_6 in the G6PD model by a factor of 2.5; details in Supplement) resulted in a value of k_H/k_D of 1.00. Simulations incorporating HK inhibition by glycerate-2,3-P_2 (Fig. 4A) and glucose-1,6-P_2 (Fig. 4B) agreed qualitatively with the dependence on these metabolites of v_{GSH} in the reconstituted system. Deviation of

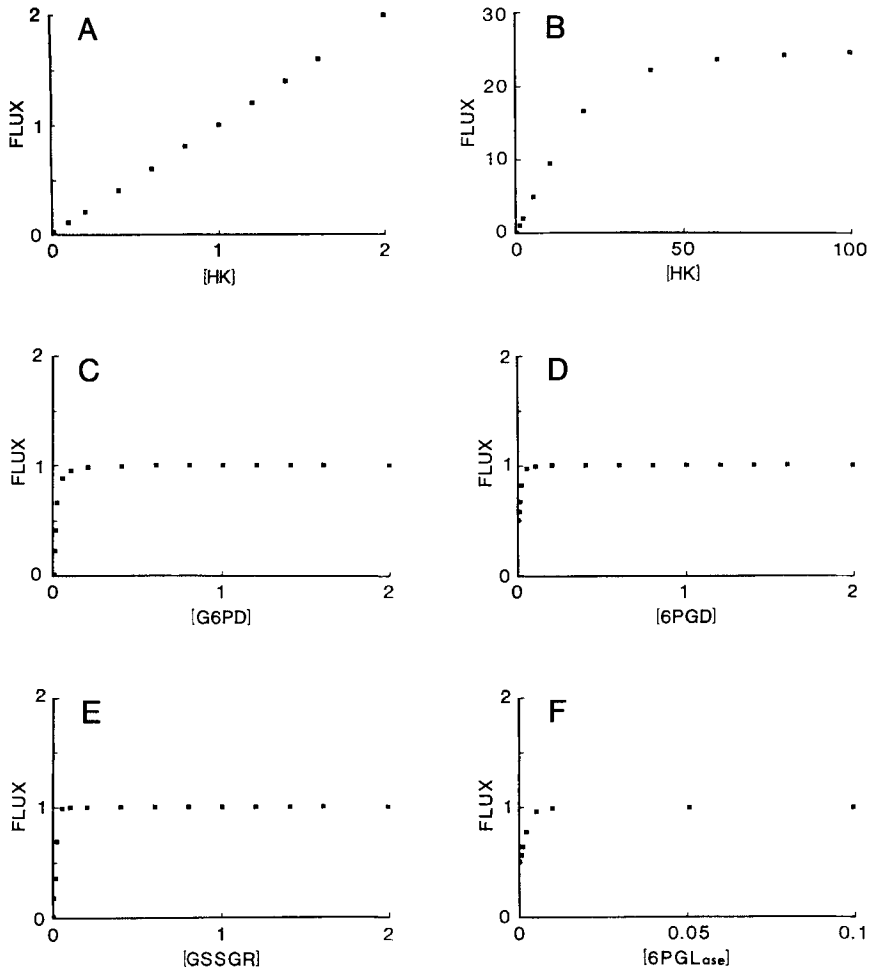

Fig. 5. *The effect on the predicted rate of GSH production (v_{GSH}) of varying the amount of each enzyme in the computer-simulation model.* Each datum represents the flux predicted by a simulation in which the activity of one reaction was varied. The concentration of each enzyme and the predicted flux are expressed relative to their values in the normal simulation system so that the point (1,1) in each figure represents the normal values of these parameters. The slope of the sensitivity profile at that point is the sensitivity coefficient of the reaction. The actual values of enzyme concentration used in the normal system were (μM): HK, 0.0163; G6PD, 0.093; gluconate-6-*P* dehydrogenase (6PGD), 2.10; GSSG reductase (GSSGR), 0.125; 6-phosphogluconolactonase (6PGLase), 14.0. The normal system value for the rate constant describing spontaneous hydrolysis of gluconolactone-6-*P* was 7.1×10^{-4} s^{-1}. All other details of the parameters used in the computer simulation are given in the Supplement. Note the different scales used in (B) and (F): the flux in (F) had a value of 1.000 at [6-phosphogluconolactonase] values greater than 0.1. The sensitivity profile for each component was calculated as described in Methods

the simulated time course from the data after about 12 min (Fig. 4A) in some cases could be due to the lability of highly purified HK at 37°C [35] or to inhibition of HK by, say, MgADP; this inhibition was not incorporated into the steady-state HK equation of [32]. In favour of the latter explanation is the observation that HK activity did not appear to decline significantly over about 20 min during the enzyme assay. Also, it is likely that MgADP accumulated to higher levels in the reconstituted system than *in situ* because of the absence or low levels of glycolytic enzymes.

Deinhibition by P_i of hexose phosphate inhibition of HK [36] was not incorporated into the simulation scheme because it has been claimed that there is no effect of P_i under simulated physiological conditions [37].

In simulations of the system in intact cells, the values of concentration of MgATP and MgADP were held constant at the reported intracellular levels of 1.44 mmol (l cell water)$^{-1}$ [24] and 0.31 mmol (l cell water)$^{-1}$ [21], respectively. In the absence of glycerate-2,3-P_2 and glucose-1,6-P_2 the predicted value of v_{GSH} was 40.43 mmol h^{-1} (l cell water)$^{-1}$. When the values of glycerate-2,3-P_2 and glucose-1,6-P_2 concentration were set to their intracellular levels (Table 9, Supplement) the estimated value of v_{GSH} was 15.4 mmol h^{-1} (l cell water)$^{-1}$ which is 1.5 times the measured rate.

The sensitivity profiles for each component in the intact cell simulation scheme are shown in Fig. 5. The sensitivity coefficient calculated for HK was 0.9948 ± 0.0025 (mean $\pm$ standard deviation of estimate); this value implies that the reaction exerts nearly full control on the simulated system and that the predicted v_{GSH} would respond almost linearly to changes in HK activity (see Fig. 5A). G6PD had a sensitivity coefficient of 0.0063 ± 0.0019 which explains the lack of an observed kinetic isotope effect on the system. The sensitivity coefficient for gluconate-6-*P* dehydrogenase was 0.0015 ± 0.0012 and the values for the lactonase reaction and GSSG reductase were less than 0.001.

DISCUSSION

The absence of a kinetic isotope effect by [1-^{2}H]glucose on v_{GSH} in intact human erythrocytes (Table 2) shows that G6PD activity is not a strong determinant of the flux of reducing equivalents in conditions of oxidative stress. This observation agrees with a previous report [6] but is a more direct demonstration since it did not involve the use of mixtures of multiple-labelled isotopic substrates and the attendant error-prone calculations. It is feasible that the G6PD reaction has a low, but significant, sensitivity coefficient for GSSG reduction in intact cells which does not result in an experimentally detectable kinetic isotope effect on v_{GSH}. In order to quantify this possibility we used the computer model to simulate the kinetic isotope effect on G6PD at higher values of the sensitivity coefficient (i.e. at lower levels of G6PD). At a sensitivity coefficient of 0.13 ($\approx$ 17 times lower G6PD concentration) the predicted value of k_H/k_D was 1.12 which should be detectable in an experiment (see values of standard deviation in Table 2); at a sensitivity coefficient of 0.18 ($\approx$ 21 times lower G6PD concentration) the predicted value was 1.19 which would be readily detectable. The absence of an observed kinetic isotope effect on v_{GSH} in intact cells therefore shows that the sensitivity coefficient of the G6PD reaction for stimulated HMS flux must be less than 0.15.

HK is the principal determinant of oxidatively stimulated flux through the HMS as was shown by the marked dependence of v_{GSH} on the concentration of glucose-1,6-P_2 in oxidatively stressed sonicate lysates supplemented with $NADP^+$ (see Table 2). It is apparent that the high $NADP^+$ concentration used in lysate experiments could have decreased the sensitivity coefficient of the G6PD reaction relative to its value in intact cells. This would lead to a more pronounced effect of glucose-1,6-P_2 on v_{GSH} in the lysate, since HK would be relatively more rate-determining, than might occur if comparable experiments could be done with intact cells. The magnitude of this change is unlikely to be great, however, since the intracellular $NADP^+$ concentration, $\approx$ 65 μmol (l cell water)$^{-1}$ [7], would be nearly saturating ($\approx$ 10 times K_m, see Supplement) for G6PD under these conditions. Also, if G6PD had a significant sensitivity coefficient in intact cells, which was decreased by high levels of $NADP^+$ in the lysate, we would expect v_{GSH} to be higher in the lysate; this was not observed (Table 2).

Morelli et al. [4] also concluded that HK was the rate-limiting step of the oxidatively stimulated HMS; the experiments involved lysed and resealed erythrocytes loaded with additional HK or G6PD. Albrecht et al. [2] studied the effect of pH and $NADP^+$ concentration on the pathway of glucose utilisation in intact cells and reached the same conclusion.

The *in situ* flux through the HMS, in the presence of high levels of GSSG, is restricted to well below the maximal capacity of the enzymes; this was shown by the severalfold difference in the value of v_{GSH} in the reconstituted system (Table 3), or with simulations of the system with effectors absent, compared to the value determined in intact cells or lysates (Table 2).

Magnani et al. [5] found no difference in the rate of the HMS under methylene blue stimulation in trisomic cells, containing 50% more HK activity than normal controls. However, all their cell incubations were done in buffer containing 27 mM P_i which favoured flux via glycolysis, rather than the HMS; this is shown by their finding that only 36% of the glucose consumption was via the HMS in control cells, with 0.5 mM methylene blue, compared with typical values of 90 – 100% found in more physiological media [2, 9]. The altered regulation of glucose consumption in the presence of high concentrations of P_i invalidates the relevance of their results to other studies of HMS flux in conditions of oxidative stress.

Gaetani et al. [3] found that the ratio (maximal rate of HMS in intact cells supplied with glucose)/(maximal activity of G6PD in haemolysate) had a value of about 1/60 in normal and G6PD-deficient cells. Since this ratio was of the same magnitude at very different G6PD activities they claimed that the enzyme was under some 'intracellular restraint' in both cell types which determined the maximal achievable HMS rate. In a later study with normal cells [8], the HMS flux in the presence of methylene blue was studied in haemolysates supplied with saturating levels of glucose-6-*P* and $NADP^+$. Since the flux in haemolysates was about 40-fold higher than that in intact cells, and comparable to the maximal G6PD activity, it was claimed that this intracellular restraint was relieved following haemolysis. These claims are incompatible since we have shown that v_{GSH} is not higher in sonicate lysates supplied with $NADP^+$ than in intact cells (Table 2). Addition of 2.5 mM glucose-6-*P* instead of glucose to such a lysate, however, allows complete GSSG reduction in less than 1 min due to the bypassing of the HK reaction and saturation of G6PD with glucose-6-*P* (data not shown); this was also predicted by our computer simulation of the system. Thus there is no good evidence that intracellular restraint of G6PD, should it exist, is relieved by haemolysis.

The apparent restraint of G6PD activity in normal erythrocytes described by Gaetani et al. [3] is explained by the low sensitivity coefficient of G6PD for stimulated HMS flux (Fig. 5C) which implies that there is a considerable excess of enzymic activity. In many forms of G6PD deficiency, young red cells have low to normal G6PD activity but older cells have negligible activity [38]; the kinetics of the enzyme may also be altered [38]. In a suspension of G6PD-deficient erythrocytes most of the G6PD activity will reside in the younger cells. The older cells in the population would have very low activities and very low flux through the HMS in response to oxidative stress. The relatively low maximal HMS rate in G6PD-deficient cells can therefore be explained by the marked heterogeneity of the cell population. Consequently, it appears probable that the similarity of the ratio of maximal HMS rate/G6PD activity in normal and G6PD-deficient cells is coincidental; the interpretation that G6PD activity limits stimulated HMS flux in normal erythrocytes [3] thus seems to be invalid.

In subsequent work, Kirkman et al. [39] revised their estimate of intracellular restraint to a value of about fivefold at high $NADP^+$: NADPH ratios. Assuming that G6PD activity was only 20% of the value used in our sensitivity analysis we recalculated a sensitivity coefficient of approximately 0.04 for the G6PD reaction. Thus even if this restraint is operative, it is apparent that G6PD activity would still not be expected to be a strong determinant of flux through the oxidatively stimulated HMS.

Kirkman et al. [39] also showed that the relationship between HMS rate (or HMS rate/G6PD activity) and the ratio $NADP^+$/NADP in intact erythrocytes was sigmoidal. Their data indicated that a maximum value of HMS rate/G6PD activity of about 0.02 was reached at $NADP^+$/NADP ratios greater than about 0.5. When we numerically simulated this experiment the relationship appeared to be hyperbolic, approaching a maximum value of HMS rate/G6PD activity of about 0.017 at $NADP^+$/NADP ratios above 0.1 – 0.2 (data

not shown). Since G6PD would not be limiting the HMS flux at higher values of $NADP^+$/NADP, the approach to a horizontal asymptote in these plots is a result of transfer of control of the HMS from G6PD to HK, rather than due to an 'intrinsic' property of G6PD as was suggested by Kirkman at al. [39]. The sigmoidal nature of the experimental data at low $NADP^+$/NADP ratios is not consistent with the predicted behaviour of the system and requires further investigation; it is, however, largely irrelevant to the regulation of the HMS at high $NADP^+$/NADP ratios.

It has been shown that GSSG reductase activity does not play an important regulatory role in limiting HMS flux under oxidative stress since the stimulated flux is normal in GSSG-reductase-deficient erythrocytes [10] and in normal cells treated with *p*-chloromercuribenzoate which reduces GSSG reductase activity to less than 10% of normal [11].

The dependence of v_{GSH} in lysates (Table 2), and in the reconstituted metabolic system (Table 3), on the concentration of glucose-1,6-P_2 supports the suggested rate-limitation of the HMS by HK under conditions of oxidative stress. Assuming that HK has a sensitivity coefficient of about 1.0 with respect to the maximal rate of GSSG reduction, one could anticipate that the magnitude of this dependence would reflect almost the full expression of glucose-1,6-P_2 inhibition of HK. It was, however, observed that comparable amounts of glucose-1,6-P_2 in lysates and the reconstituted system caused a greater percentage of inhibition of v_{GSH} than of HK in the assay medium. This paradox may be resolved by considering the interactions between glucose-1,6-P_2, Mg^{2+} and P_i and their effects on HK activity.

Rose et al. [40] found that the value of the inhibition constant of HK (type II) for glucose-1,6-P_2 increased three-fold when the concentration of free Mg^{2+} was increased from 0.5 mM to 5.0 mM. Assuming that Mg^{2+} · glucose-1,6-P_2 was not inhibitory, they calculated a value of about 2.5 mM for the dissociation constant, K_d, of the complex.

We calculated the concentrations of free glucose-1,6-P_2 (assuming K_d = 2.5 mM) in the HK assay medium and reconstituted metabolic system and found an equivalent effect on assayed HK activity and v_{GSH} by the same concentration of free glucose-1,6-P_2. This is consistent with virtually full expression of the HK inhibition on the flux of reducing equivalents to GSSG in this system.

The dependence of v_{GSH} in the lysate on the calculated concentration of free glucose-1,6-P_2 was not as marked as in the reconstituted system. This can be explained by the physiological (1 mM) concentration of P_i in the lysate raising the value of the apparent inhibition constant of HK for glucose-1,6-P_2.

Deinhibition by P_i of hexose phosphate inhibition of erythrocyte HK has been widely reported [36, 41–43] although not all of these studies were done under conditions close to physiological. In contrast, Gerber et al. [37] found no effect of P_i concentrations up to 10 mM in simulated physiological conditions. Our studies support the suggestion that physiological concentrations of P_i cause deinhibition of glucose-1,6-P_2 inhibition of HK under physiological conditions (Table 3).

Reported values of K_i (glucose-1,6-P_2) for HK have been estimated at concentrations of free Mg^{2+} of about 5 mM [36, 37, 43]. Under these conditions most of the glucose-1,6-P_2 is complexed and the estimated value of K_i is therefore an overestimate since it is the free form which appears to be inhibitory. Since the concentration of Mg^{2+} in intact cells is reported to be about 0.7 mM [24], in the future it will be necessary to have accurate estimates of K_d (Mg-glucose-1,6-P_2) and K_i (free glucose-1,6-P_2) for incorporation into a computer model before it will be able to describe more adequately the kinetic behaviour of HK. It will also be necessary to determine the effect of physiological concentrations of P_i on raising the apparent K_i (free glucose-1,6-P_2) of HK under physiological conditions.

These considerations have been ignored in previous simulations of glycolysis and the HMS [16, 17, 24]. The models have used descriptive rate laws for each enzymic reaction and, for example, have neither incorporated inhibition of HK by glucose-1,6-P_2 nor the complexities of P_i deinhibition and Mg^{2+} ·glucose-1,6-P_2 interaction. Although the predictions of these models have agreed qualitatively with experimental data it appears that the quantitative understanding of the factors controlling erythrocyte glucose metabolism is not as adequate as had previously been thought. It appears likely (see Fig. 8C in the Supplement) that the physiological concentration of glucose-1,6-P_2 is more important than glucose-6-*P* in limiting both the normal rate of glucose utilisation and the capacity of the erythrocyte to produce reducing equivalents in response to oxidative challenge.

Several other factors, which may be considered to influence the rate of GSSG reduction, were also not included in the computer model: transport of glucose into the red cell is very rapid [1] and would not limit the rate of glucose utilisation; efflux of GSSG from cells during the time of our experiments is negligible ($\approx 1\%$); competition by glycolysis for glucose-6-*P* formed via HK accounts for less than 10% of the total glucose utilisation at high ratios of $NADP^+$:NADP [2, 9], thus we considered it was not a gross oversimplification to omit a complex glycolytic scheme from the simulation.

Finally, it has been estimated that about 30% of the flux through the oxidatively stimulated HMS is from recycled glucose-6-*P* rather than glucose-6-*P* formed directly via the HK reaction [45, 46]. This flux does not occur in the reconstituted metabolic system and was not incorporated into the computer simulation scheme. In future, when the realistic effects of glucose-1,6-P_2, Mg^{2+} and P_i are incorporated into the HK model the simulations of the intact cell should underestimate v_{GSH} by about 30% (in the absence of recycling). If the simulations were still to predict a value of v_{GSH} significantly faster than this then, given the low sensitivity coefficients of the other reactions, we would infer that the HK reaction was subject to inhibition by still other effectors. Such a finding would not, however, alter the validity of our claim that almost complete control of the oxidatively stimulated flux through the HMS is exerted by HK.

The work was supported by the Australian National Health and Medical Research Council and D. R. T. received a Commonwealth Postgraduate Research Scholarship. Mr B. T. Bulliman is thanked for his contribution to the computing.

REFERENCES

1. Grimes, A. J. (1980) *Human red cell metabolism* pp. 192–258, Blackwell Scientific Publications, Oxford.
2. Albrecht, V., Roigas, H., Schultze, M., Jacobasch, G. R. & Rapoport, S. (1971) *Eur. J. Biochem. 20*, 44–50.
3. Gaetani, G. D., Parker, J. C. & Kirkman, H. N. (1974) *Proc. Natl Acad. Sci. USA 71*, 3584–3587.
4. Morelli, A., Benatti, U., Salamino, F., Sparatore, B., Michetti, M., Melloni, E., Pontremoli, S. & De Flora, A. (1979) *Arch. Biochem. Biophys. 197*, 543–550.

5. Magnani, M., Stocchi, V., Piatti, E., Dacha, M., Dallapiccola, B. & Fornaini, G. (1983) *Blood 61*, 915–919.
6. Rose, I. A. (1961) *J. Biol. Chem. 236*, 603–609.
7. Omachi, A., Scott, C. B. & Hegarty, H. (1969) *Biochim. Biophys. Acta 184*, 139–147.
8. Galiano, S., Mareni, C. & Gaetani, G. D. (1978) *Biochim. Biophys. Acta 501*, 1–9.
9. Roigas, H., Zoellner, E., Jacobasch, G., Schultze, M. & Rapoport, S. (1970) *Eur. J. Biochem. 12*, 24–30.
10. Paniker, N. V., Srivastava, S. K. & Beutler, E. (1970) *Biochim. Biophys. Acta 215*, 456–460.
11. Benohr, H. Chr. & Waller, H. D. (1974) in *Glutathione* (Flohe, L., Benohr, H. Chr., Sies, S., Waller, H. D. & Wendel, A., eds) pp. 184–191, Georg Thieme, Stuttgart.
12. Scopes, R. K. (1973) *Biochem. J. 134*, 197–208.
13. Eschrich, K., Schellenberger, W. & Hofmann, E. (1982) *Acta Biol. Med. Germ. 41*, 415–424.
14. Kacser, H. & Burns, J. A. (1973) in *Rate control of biological processes* (Davies, D. D., ed.) pp. 65–104, Cambridge University Press, London.
15. Heinrich, R. & Rapoport, T. A. (1974) *Eur. J. Biochem. 42*, 89–95.
16. Kothe, K., Sachsenroder, Ch. & Reich, J. G. (1975) *Acta Biol. Med. Germ. 34*, 203–228.
17. Ataullakhanov, F. I., Buravtsev, V. N., Zhabotinskii, A. M., Norina, S. B., Pichugin, A. V. & Erlikh, L. I. (1981) *Biokhimiya 46*, 723–731.
18. York, M. J., Kuchel, P. W., Chapman, B. E. & Jones, A. J. (1982) *Biochem. J. 207*, 65–72.
19. King, G. F. & Kuchel, P. W. (1984) *Biochem. J. 220*, 553–560.
20. Srivastava, S. K., Awasthi, Y. C. & Beutler, E. (1974) *Biochem. J. 139*, 289–295.
21. Beutler, E. (1975) *Red cell metabolism: a manual of biochemical methods* 2nd edn, Grune and Stratton, New York.
22. van Kampen, E. J. & Zijlstra, W. G. (1961) *Clin. Chim. Acta 6*, 538–544.
23. Hickey, T. M., Uddin, D. E. & Kiesow, L. A. (1979) *Clin. Chem. 25*, 1314–1317.
24. Gerber, G., Berger, H., Janig, G.-R., Ruckpaul, K. & Rapoport, S. M. (1975) in *VII. Internationales Symposium über Struktur und Funktion der Erythrozyten* (Rapoport, S. M. & Jung, F., eds) pp. 275–282, Akademie-Verlag, Berlin.
25. Fersht, A. (1977) *Enzyme structure and mechanism*, pp. 126–133, Freeman, San Francisco.
26. Roman, G.-C. & Garfinkel, D. (1978) *Comput. Biomed. Res. 11*, 3–15.
27. Berger, H., Janig, G.-R., Gerber, G., Ruckpaul, K. & Rapoport, S. M. (1973) *Eur. J. Biochem. 38*, 553–562.
28. Perrin, D. D. & Sayce, I. G. (1967) *Talanta 14*, 833–842.
29. Endre, Z. H., Kuchel, P. W. & Chapman, B. E. (1984) *Biochim. Biophys. Acta 803*, 137–144.
30. Reimann, B., Kuttner, G., Maretzki, D. & Rapoport, S. (1975) *Acta Biol. Med. Germ. 34*, 1777–1785.
31. Bartlett, G. R. (1968) *Biochim. Biophys. Acta 156*, 231–239.
32. Kuchel, P. W., Chapman, B. E., Lovric, V. A., Raftos, J. E., Stewart, I. M. & Thorburn, D. R. (1984) *Biochim. Biophys. Acta 805*, 191–203.
33. Bauer, H. P., Srihari, T., Jochims, J. C. & Hofer, H. W. (1983) *Eur. J. Biochem. 133*, 163–168.
34. Horecker, B. L. & Smyrniotis, P. Z. (1953) *Biochim. Biophys. Acta 12*, 98–102.
35. Rijksen, G. & Staal, G. E. J. (1976) *Biochim. Biophys. Acta 445*, 330–341.
36. Stocchi, V., Magnani, M., Canestrari, F., Dacha, M. & Fornaini, G. (1982) *J. Biol. Chem. 257*, 2357–2364.
37. Gerber, G., Preissler, H., Heinrich, R. & Rapoport, S. M. (1974) *Eur. J. Biochem. 45*, 39–52.
38. Luzzatto, L. (1974) *Br. J. Haematol. 28*, 151–155.
39. Kirkman, H. N., Wilson, W. G. & Clemons, E. H. (1980) *J. Lab. Clin. Med. 95*, 877–887.
40. Rose, I. A., Warms, J. V. B. & Kosow, D. P. (1974) *Arch. Biochem. Biophys. 164*, 729–735.
41. Kosow, D. P., Oski, F. A., Warms, J. V. B. & Rose, I. A. (1973) *Arch. Biochem. Biophys. 157*, 114–124.
42. Rijksen, G. & Staal, G. E. J. (1977) *Biochim. Biophys. Acta 485*, 75–86.
43. Rijksen, G., Jansen, G., Kraaijenhagen, R. J., van der Vlist, M J. M., Vlug, A. M. C. & Staal, G. E. J. (1981) *Biochim. Biophys Acta 659*, 292–301.
44. Heinrich, R., Rapoport, S. M. & Rapoport, T. A. (1977) *Prog Biophys. Mol. Biol. 32*, 1–82.
45. Szeinberg, A. & Marks, P. A. (1961) *J. Clin. Invest. 40*, 914–924
46. Davidson, W. D. & Tanaka, K. R. (1972) *Br. J. Haematol. 23* 371–385.
47. Warburg, O. & Christian, W. (1941) *Biochem. Z. 310*, 384–421.
48. De Flora, A., Giuliano, F. & Morelli, A. (1973) *Ital. J. Biochem 22*, 258–270.
49. Pearse, M. F. & Rosemeyer, M. A. (1974) *Eur. J. Biochem. 42*, 213–223.
50. Mannervik, B., Jacobsson, K. & Boggaram, V. (1976) *FEBS Lett 66*, 221–224.
51. Soldin, S. J. & Balinsky, D. (1968) *Biochemistry 7*, 1077–1081.
52. Kanji, M. I., Toews, M. L. & Carper, W. R. (1976) *J. Biol. Chem. 251*, 2258–2262.
53. Indge, K. J. & Childs, R. E. (1976) *Biochem. J. 155*, 567–570.
54. Cohen, P. & Rosemeyer, M. A. (1975) *Methods Enzymol. 41*, 208–214.
55. Cohen, P. & Rosemeyer, M. A. (1969) *Eur. J. Biochem. 8*, 1–7.
56. Glaser, L. & Brown, D. H. (1955) *J. Biol. Chem. 216*, 67–79.
57. Northrop, D. B. (1977) in *Isotope effects on enzyme-catalyzed reactions* (Cleland, W. W., O'Leary, M. H. & Northrop, D. B., eds) p. 294, Plenum Press, New York.
58. Villet, R. H. & Dalziel, K. (1972) *Eur. J. Biochem. 27*, 251–258.
59. Pearse, B. M. F. & Rosemeyer, M. A. (1974) *Eur. J. Biochem. 42*, 225–235.
60. Villet, R. H. & Dalziel, K. (1969) *Biochem. J. 115*, 633–638.
61. Staal, G. E. J. & Veeger, C. (1969) *Biochim. Biophys. Acta 185*, 49–62.
62. Mannervik, B. (1973) *Biochem. Biophys. Res. Commun. 53*, 1151–1158.
63. Worthington, D. J. & Rosemeyer, M. A. (1976) *Eur. J. Biochem. 67*, 231–238.
64. Krohne-Ehrich, G., Schirmer, R. H. & Untucht-Grau, R. (1977) *Eur. J. Biochem. 80*, 65–71.
65. Worthington, D. J. & Rosemeyer, M. A. (1975) *Eur. J. Biochem. 60*, 459–466.
66. Scott, E. M., Duncan, I. W. & Ekstrand, V. (1963) *J. Biol. Chem. 238*, 3928–3933.
67. Schofield, P. J. & Sols, A. (1975) *Biochem. Biophys. Res. Commun. 71*, 1313–1318.
68. McGilvery, R. W. (1979) *Biochemistry, a functional approach*, 2nd edn, p. 756, W. B. Saunders Company, Philadelphia.

Supplementary material to

Regulation of the human erythrocyte hexose monophosphate shunt

A study using NMR spectroscopy, a kinetic isotope effect, a reconstituted system and computer simulation

David R. THORBURN and Philip W. KUCHEL

ENZYME PREPARATIONS

During the purifications, protein content was estimated from the absorbance at 260 nm and 280 nm assuming that a protein concentration of 1 mg $(ml)^{-1}$ has an absorbance of 1.0 at 280 nm [47]. The following buffers were used.

Buffer A: 50 mM sodium phosphate with 1 mM EDTA, 1 mM 6-amino-*n*-hexanoic acid, 0.1% (v/v) 2-mercaptoethanol, pH 7.6.

Buffer B: 50 mM Hepes with 130 mM KCl, 1 mM EDTA, 1 mM 6-amino-*n*-hexanoic acid, 0.1% (v/v) 2-mercaptoethanol, pH 7.2 at 37 °C.

Buffer C: 5 mM sodium potassium phosphate with 5 mM glucose, 3 mM KF, 3 mM 2-mercaptoethanol, 9% (v/v) glycerol, pH 7.5.

Purification of glucose-6-phosphate dehydrogenase, gluconate-6-phosphate dehydrogenase and GSSG reductase

The procedure used was based on several published methods [48–50].

Preparation of haemolysate. Fresh (1-day-old) human erythrocytes in citrate/phosphate/dextrose medium were washed three times with 3 vol. glucose 5 mmol l^{-1} in physiological saline. Cells were lysed by addition of 1–3 vol. ice-cold 1% toluene, 7 mM EDTA, 4 mM 2-mercaptoethanol, followed by vigorous shaking for 10 min. The lysate was centrifuged at $2000 \times g$ for 30 min after which the upper toluene layer was removed. The clear haemolysate was recovered; all subsequent procedures were performed at 4 °C.

Affinity chromatography. The 'stroma-free' lysate (500 ml) was applied to a 2′,5′-ADP-Sepharose 4B column (2.2 × 9.5 cm), equilibrated with buffer A, at a flow rate of about 20 ml h^{-1}. After the sample had been applied, approximately 10 bed volumes of NaCl 25 mmol l^{-1} in buffer A was passed through the column. The following 'pulses' of reagent mixtures in buffer A were then applied to the column, separated by one to four bed volumes of NaCl 25 mmol l^{-1} in buffer A: (a) 40 ml 0.1 mM $NADP^+$, (b) 25 ml 0.2 mM $NADP^+$, (c) 40 ml 10 mM $NADP^+$ and (d) 40 ml 1 mM GSH, 1 mM NADPH. Most of the G6PD activity was eluted after the first pulse (a). The active fractions were pooled and concentrated to about 1 ml by ultrafiltration using a PM30 membrane (50-ml chamber) followed by a PM10 membrane (10-ml chamber). The G6PD preparation was then exchanged into $NADP^+$ 10 μmol l^{-1} in buffer B using a Pharmacia PD10 Sephadex G-25 column (1.5 × 5.2 cm). Pulse b eluted most of the remaining G6PD but less than 10% of the total of the other two enzymes. The specific activity of the purified G6PD was 13.9 units mg^{-1} (1480-fold purification, 44% yield).

Pulse c eluted the bulk of the gluconate-6-*P* dehydrogenase activity and, with one batch of gel, about 90% of the GSSG reductase activity. In other experiments with a different batch of gel we found that most of the GSSG reductase activity remained bound to the column under these conditions; it was only eluted following pulse d. Column fractions were made 10 mM in FAD prior to assaying for GSSG reductase, since this moiety apparently dissociated from the enzyme during the purification.

Ammonium sulphate fractionation. Active fractions eluted by pulse c were pooled and concentrated using a PM30 membrane. This pool was then brought to 55% saturation with ammonium sulphate by the slow addition of the solid salt. After 2 h gentle stirring, the suspension was centrifuged ($10000 \times g$, 20 min) and the supernatant solution (containing gluconate-6-*P* dehydrogenase) was brought to 75% saturation by further addition of the solid salt. Following overnight precipitation, the suspension was centrifuged as before and the precipitate was redissolved in $NADP^+$ (10 μmol l^{-1}) in buffer A and dialysed against 200 vol. of the same solution for about 9 h with two changes of fresh buffer. The gluconate-6-*P* dehydrogenase preparation was made 25% saturated with ammonium sulphate and bovine serum albumin 1 mg ml^{-1} was added; the preparation was exchanged into $NADP^+$ (10 μmol l^{-1}) in buffer B using a PD10 column just prior to use. The specific activity of the purified gluconate-6-*P* dehydrogenase was 16.1 units mg^{-1} (1940-fold purification, 18.4% yield).

GSSG reductase was prepared either from the 55% ammonium sulphate pellet (when eluted by pulse c) or from the pooled and concentrated active fractions eluted by pulse d. The GSSG reductase preparation was then exchanged into buffer B using a PD10 column; the final specific activity was 31.2 units mg^{-1} (4970-fold purification, 83.6% yield).

Purification of hexokinase

The initial steps of the HK purification involving saponin lysis of washed cells, batch treatment with DEAE-Sephadex A-50 and ammonium sulphate fractionation were the same as used by Stocchi et al. [36] and resulted in a purification factor of about 32-fold. The HK preparation was then passed through a 2′,5′-ADP-Sepharose 4B column (2.2 × 9.5 cm) equilibrated with buffer C and the column was washed with several bed volumes of NaCl (25 mmol l^{-1}) in buffer C. Under these conditions the bulk of the HK activity remained bound to the column and was not eluted by a 25-ml pulse of $NADP^+$ (5 mmol l^{-1}), NADPH (1 mmol l^{-1}), GSH (1 mmol l^{-1}) in buffer C which eluted most of the other three enzyme activities. KCl (1 mol l^{-1}) in buffer C eluted the HK activity; active fractions were pooled and brought to 80% saturation with solid ammonium sulphate. After 2 h gentle stirring, the suspension was centrifuged ($10000 \times g$, 20 min) and the precipitate redissolved in buffer C and subsequently dialysed (12 h with two changes) against 200 vol. buffer C. The retentate was centrifuged ($16000 \times g$, 20 min) and the supernatant solution was concentrated using a PM10 membrane prior to transfer to buffer B supplemented with 3 mM KF, 5 mM glucose and 9% (v/v) glycerol. The specific activity of the purified HK was 0.355 unit mg^{-1} (480-fold purification, 18.4% yield). Table 4 shows the contamination of each preparation with the other enzyme activities and the volumes of each preparation used to achieve the desired activities in a typical reconstitution experiment.

COMPUTER SIMULATIONS

Hexokinase

The HK model used in the computer simulations has been presented previously [32].

Glucose-6-phosphate dehydrogenase

The mechanism of human erythrocyte G6PD has been reported to be either of compulsory order, with the cofactor binding first and released last, or of a random nature [39, 51]. The lability of 6-phosphogluconolactone in aqueous solution has precluded the complete kinetic analysis of the enzyme but studies with the mammalian liver enzyme [52] support an ordered sequential mechanism and we assumed this also held for the erythrocyte enzyme. The mechanism

Table 4. *Activities of each enzyme in the various preparations used in a typical reconstitution experiment*
The activities of each of the assayed enzymes in the four enzyme preparations is given together with the final activity of each enzyme needed to prepare a reconstituted system. The volume of each preparation needed to achieve the set of final activities in a 1.0-ml enzyme system was calculated by solving the four simultaneous equations as described in the Methods. 6PGD = gluconate-6-*P* dehydrogenase, GSSGR = GSSG reductase

Preparation	Enzyme activity				Volume of preparation
	HK	G6PD	6PGD	GSSGR	
	units ml^{-1}				µl
HK	1.88	4.10	0.363	0.950	27.66
G6PD	0.0	39.21	0.0	0.0	16.71
6PGD	0.0	0.032	5.75	0.121	154.30
GSSGR	0.0	0.178	0.156	103.5	5.25
Final	0.052	0.774	0.898	0.588	203.9

used (Fig. 6A) included the chemical conversion of ternary complexes to facilitate the simulation of a kinetic isotope effect (see later). The algorithm of Indge and Childs [53] was used to derive the steady-state rate equation for G6PD (and for gluconate-6-*P* dehydrogenase and GSSG reductase) which was:

$$\frac{d[P]}{dt} = \frac{(N_1[A][B]-N_2[P][Q])[E_t]}{(D_1 + D_2[A] + D_3[B] + D_4[P] + D_5[Q] + D_6[A][B] + D_7[A][P] + D_8[B][Q] + D_9[P][Q] + D_{10}[A][B][P] + D_{11}[B][P][Q])} \quad (1)$$

where
$N_1 = k_1k_3k_5k_7k_9$
$N_2 = k_2k_4k_6k_8k_{10}$
$D_1 = k_2k_9(k_4k_6+k_5k_6+k_5k_7)$
$D_2 = k_1k_9(k_4k_6+k_5k_6+k_5k_7)$
$D_3 = k_3k_5k_7k_9$
$D_4 = k_2k_4k_6k_8$
$D_5 = k_2k_{10}(k_4k_6+k_5k_6+k_5k_7)$
$D_6 = k_1k_3(k_5k_7+k_5k_9+k_6k_9+k_7k_9)$
$D_7 = k_1k_4k_6k_8$
$D_8 = k_3k_5k_7k_{10}$
$D_9 = k_8k_{10}(k_2k_4+k_2k_5+k_2k_6+k_4k_6)$
$D_{10} = k_1k_3k_8(k_5+k_6)$
$D_{11} = k_3k_8k_{10}(k_5+k_6)$

The symbols relate to the annotation used in Fig. 6A and $[E_t]$ is the total enzyme concentration. The following steady-state kinetic parameters can then be derived: $K = N_1/N_2$, $k_{cat} = N_1/D_6$, $K_m^A = D_3/D_6$, $K_m^B = D_2/D_6$. Inhibition by Q (NADPH) is competitive with A ($NADP^+$) and the inhibition constant $K_i^Q = D_3/D_8$.

Several authors [39, 51, 54] have reported values of the kinetic parameters of the human erythrocyte enzyme. The values we used were those estimated under conditions closest to physiological (Krebs Ringer/Tes buffer, pH 7.4, I = 0.15 M, 25°C) [39] and are given in Table 5. The enzyme concentration and k_{cat} were calculated as follows.

The specific activity of the most highly purified (72000-fold) human erythrocyte enzyme is 220 µmol min^{-1} mg^{-1} (I = 0.1 M, pH 9.0, 25°C) [54], which is equivalent to a value of 394 µmol min^{-1} mg^{-1} when corrected for 37°C according to [21]. Assuming that the predominant active molecular form of the enzyme in the red cell is a dimer of relative molecular mass 105000 [54], we can calculate a turnover number of 689 s^{-1}; from the measured human erythrocyte G6PD activity of 3870 µmol min^{-1} (l cell water)$^{-1}$ (Table 1) this corresponds to an enzyme concentration of 93 nmol (l cell water)$^{-1}$ for the dimer. Although the value of k_{cat} may have been slightly overestimated (G6PD activity at pH 7.4 is only about 80% of that at pH 9.0 [55]) this is compensated for by calculating the enzyme concentration from the activity measured under simulated physiological conditions.

The value of the equilibrium constant of the reaction,

$$K = \frac{[\text{gluconolactone-6-}P][NADPH][H^+]}{[\text{glucose-6-}P][NADP^+]},$$

has been reported to be 0.6 µM at 28°C [56]. This corresponds to a value of $K/[H^+]$ of 9.5 at pH 7.2.

Rose [6] reported on the magnitude of the kinetic isotope effect on human erythrocyte G6PD when glucose-6-*P* was replaced by [1-^{2}H]glucose-6-*P*. At high substrate concentration ^DV = 2.4 while at low substrate concentration $^DV/K$ = 1.4; this uses the nomenclature of Northrop [57]. The simulated isotope effect was invoked in the G6PD model by decreasing the values of the two rate constants involved in the central isomerisation process (k_5 and k_6, Fig. 6A) by a factor of 2.5. The model then predicted the reported values of ^DV and $^DV/K$ without changing K.

Gluconate-6-phosphate dehydrogenase

The mechanism of human erythrocyte gluconate-6-*P* dehydrogenase was assumed to be the same as for the sheep liver enzyme which has a compulsory order mechanism [58] as shown in Fig. 6B. The derived steady-state rate-equation was:

$$\frac{d[R]}{dt} = \frac{(N_1[A][B]-N_2[P][Q][R])[E_t]}{\begin{aligned}&(D_1 + D_2[A] + D_3[B] + D_4[P] + D_5[R] + D_6[A][B] + D_7[A][P] + D_8[B][R] + D_9[P][Q]\\ &+ D_{10}[P][R] + D_{11}[Q][R] + D_{12}[A][B][P] + D_{13}[A][B][Q] + D_{14}[A][P][Q] + D_{15}[B][Q][R]\\ &+ D_{16}[P][Q][R] + D_{17}[A][B][P][Q] + D_{18}[B][P][Q][R])\end{aligned}} \quad (2)$$

where
$N_1 = k_1k_3k_5k_7k_9k_{11}$
$N_2 = k_2k_4k_6k_8k_{10}k_{12}$
$D_1 = k_2k_9k_{11}(k_4k_6+k_4k_7+k_5k_7)$
$D_2 = k_1k_9k_{11}(k_4k_6+k_4k_7+k_5k_7)$
$D_3 = k_3k_5k_7k_9k_{11}$
$D_4 = k_2k_4k_6k_8k_{11}$
$D_5 = k_2k_9k_{12}(k_4k_6+k_4k_7+k_5k_7)$
$D_6 = k_1k_3(k_5k_9k_{11}+k_6k_9k_{11}+k_7k_9k_{11}+k_5k_7k_9+k_5k_7k_{11})$
$D_7 = k_1k_4k_6k_8k_{11}$
$D_8 = k_3k_5k_7k_9k_{12}$
$D_9 = k_2k_4k_6k_8k_{10}$
$D_{10} = k_2k_4k_6k_8k_{12}$
$D_{11} = k_2k_{10}k_{12}(k_4k_6+k_4k_7+k_5k_7)$
$D_{12} = k_1k_3k_8k_{11}(k_5+k_6)$
$D_{13} = k_1k_3k_5k_7k_{10}$
$D_{14} = k_1k_4k_6k_8k_{10}$
$D_{15} = k_3k_5k_7k_{10}k_{12}$
$D_{16} = k_8k_{10}k_{12}(k_2k_4+k_2k_5+k_2k_6+k_4k_6)$
$D_{17} = k_1k_3k_8k_{10}(k_5+k_6)$
$D_{18} = k_3k_8k_{10}k_{12}(k_5+k_6)$

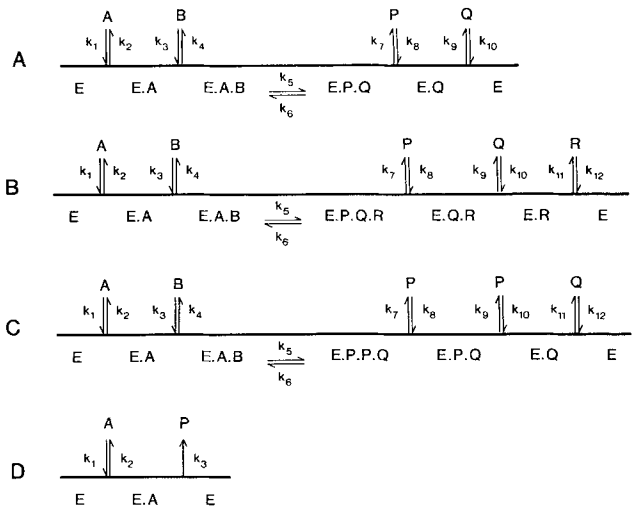

Fig. 6. *Steady-state kinetic mechanisms assumed for the reactions in the simulation scheme.* (A) G6PD reaction. Symbols: A, $NADP^+$; B, glucose-6-*P*; P, gluconolactone-6-*P*; Q, NADPH. (B) Gluconate-6-*P* dehydrogenase reaction. Symbols: A, $NADP^+$; B, gluconate-6-*P*; P, CO_2; Q, ribulose-5-*P*; R, NADPH. (C) GSSG reductase reaction. Symbols: A, NADPH; B, GSSG; P, GSH; Q, $NADP^+$. (D) 6-Phosphogluconolactonase reaction. Symbols: A, gluconolactone-6-*P*; P, gluconate-6-*P*. E represents the free enzyme in each mechanism and all other species are the corresponding enzyme-metabolite complexes

The symbols relate to the annotation used in Fig. 6B and $[E_t]$ is the total enzyme concentration. The form of the expressions for K, k_{cat}, K_m^A and K_m^B are the same as for G6PD but the compound numerator and denominator terms are those given above. Inhibition by R (NADPH) is competitive with A ($NADP^+$) and $K_i^R = D_3/D_8$.

The kinetic parameters of the human erythrocyte enzyme have been estimated at pH 8.0, I = 0.1 M, 25°C [49] and are given in Table 6. The specific activity of the most highly purified (5000-fold) human erythrocyte enzyme is 10.0 μmol min^{-1} mg^{-1} under these conditions [49] which is equivalent to a value of 20.6 μmol min^{-1} mg^{-1} when corrected for 37°C according to [21]. Since the enzyme exists predominantly as a dimer of relative molecular mass 104000 [59] the corresponding k_{cat} is 35.7 s^{-1}. Given that the erythrocyte gluconate-6-*P* dehydrogenase activity is 4490 μmol min^{-1} (l cell water)$^{-1}$ (Table 1), the erythrocyte enzyme concentration is 2.10 μmol (l cell water)$^{-1}$.

The equilibrium constant of the reaction,

$$K = \frac{[CO_2][\text{ribulose-5-}P][NADPH]}{[\text{gluconate-6-}P][NADP^+]},$$

has a value of 0.170 M (pH 6.95, I = 0.12 M, 38°C) which is reported to be independent of pH and ionic strength in the ranges 6.5–7.9 and 0.04–0.45 M, respectively [60].

GSSG reductase

The steady-state kinetics of GSSG reductase from a variety of sources, including the human erythrocyte [61, 62], are consistent with the enzyme operating by a branched mechanism involving loops corresponding to one ping-pong and one sequential mechanism. It has been claimed [62] that the sequential and ping-pong mechanisms dominate at high and low concentrations of GSSG, respectively. The GSSG concentration remains relatively high during the bulk of the GSSG reduction time course in cells treated with *t*-butyl hydroperoxide and we have, thus, made the simplifying assumption that the enzyme operates by the sequential mechanism as shown in Fig. 6C. The derived steady-state rate equation was:

Table 5. *Kinetic parameters used in the G6PD model*
The reported values of some steady-state kinetic parameters of human erythrocyte G6PD which have been estimated under conditions closest to physiological are given. The set of unitary rate constants for the model described in Fig. 6A that yield the predicted values of these parameters is: $k_1 = 1.1\times10^8$ M^{-1} s^{-1}, $k_3 = 0.26\times10^8$ M^{-1} s^{-1}, $k_8 = 11\times10^8$ M^{-1} s^{-1}, $k_{10} = 14\times10^8$ M^{-1} s^{-1}; $k_2 = 0.87\times10^3$ s^{-1}, $k_4 = 0.30\times10^3$ s^{-1}, $k_5 = 0.75\times10^3$ s^{-1}, $k_6 = 2.0\times10^3$ s^{-1}, $k_7 = 220\times10^3$ s^{-1}, $k_9 = 10\times10^3$ s^{-1}

Parameter	Predicted value	Literature value
$K_m^{NADP^+}$	6.27 μM	6.51 ± 0.61 μM [39]
$K_m^{glucose\text{-}6\text{-}P}$	37.2 μM	38.3 ± 3.6 μM [39]
$K_s^{NADP^+}$	7.91 μM	7.91 ± 1.45 μM [39]
K_i^{NADPH}	7.14 μM	7.11 ± 1.29 μM [39]
$K_i^{gluconolactone\text{-}6\text{-}P}$	79 μM	–[a]
$K/[H^+]$	5.9	9.5 [56]
k_{cat}	690 s^{-1}	689[b] s^{-1}

[a] The inhibition constant for gluconolactone-6-*P* has not been measured due to the instability of the lactone in aqueous solution.
[b] Derived in text.

Table 6. *Kinetic parameters used in the gluconate-6-*P *dehydrogenase model*
The reported values for some steady-state kinetic parameters of human erythrocyte gluconate-6-*P* dehydrogenase are given. The set of unitary rate constants for the model described in Fig. 6B that yield the predicted values of these parameters is: $k_1 = 1.2\times10^6$ M^{-1} s^{-1}, $k_3 = 10^7$ M^{-1} s^{-1}, $k_8 = 0.036\times10^6$ M^{-1} s^{-1}, $k_{10} = 0.45\times10^6$ M^{-1} s^{-1}, $k_{12} = 9.9\times10^6$ M^{-1} s^{-1}; $k_2 = 4.1\times10^2$ s^{-1}, $k_4 = 2.6\times10^4$ s^{-1}, $k_5 = 0.48\times10^2$ s^{-1}, $k_6 = 0.30\times10^2$ s^{-1}, $k_7 = 6.3\times10^2$ s^{-1}, $k_9 = 8.0\times10^2$ s^{-1}, $k_{11} = 3.0\times10^2$ s^{-1}

Parameter	Predicted value	Literature value
$K_m^{NADP^+}$	29.8 μM	30 μM [49]
$K_m^{gluconate\text{-}6\text{-}P}$	20.3 μM	20 μM [49]
K_i^{NADPH}	30.3 μM	30 μM [49]
$K_i^{ribulose\text{-}5\text{-}P}$	1.8 mM	–[a]
$K_i^{CO_2}$	17.5 mM	–[a]
K	0.17 M	0.17 M [60]
k_{cat}	35.7 s^{-1}	35.7[b] s^{-1}

[a] Values of the inhibition constants of erythrocyte gluconate-6-*P* dehydrogenase for ribulose-5-*P* and CO_2 have not been reported.
[b] Derived in text.

where the numerator and denominator terms (N_1, N_2 and D_1-D_{18}) are the same compound formulations of rate constants as in Eqn (2) and the symbols relate to the annotation used in Fig. 6C. $[E_t]$ is the total active enzyme concentration. The expressions, in terms of the rate constants, for K, k_{cat}, K_m^A and K_m^B are identical to those for gluconate-6-*P* dehydrogenase while inhibition by Q ($NADP^+$) is competitive with A (NADPH) and $K_i^Q = D_3/D_8$.

The kinetic parameters of the human erythrocyte enzyme have been estimated at pH 7.0, I = 0.3 M, 25°C [63] and are given in Table 7. The specific activity of the most highly purified human erythrocyte enzyme (64000-fold) was 236 μmol min^{-1} mg^{-1} under nearly identical conditions [64] which is equivalent to a value of 435 μmol min^{-1} mg^{-1} when corrected for 37°C according to [21]. The enzyme exists predominantly as a dimer of relative molecular

$$\frac{d[Q]}{dt} = \frac{(N_1[A][B]-N_2[P]^2[Q])[E_t]}{\begin{aligned}&(D_1 + D_2[A] + D_3[B] + D_4[P] + D_5[Q] + D_6[A][B] + D_7[A][P] + D_8[B][Q]\\&+ D_9[P]^2 + (D_{10} + D_{11})[P][Q] + (D_{12} + D_{13})[A][B][P] + D_{14}[A][P]^2 + D_{15}[B][P][Q]\\&+ D_{16}[P]^2[Q] + D_{17}[A][B][P]^2 + D_{18}[B][P]^2[Q])\end{aligned}} \quad (3)$$

Table 7. *Kinetic parameters used in the GSSG reductase model*
The reported values for some steady-state kinetic parameters of human erythrocyte GSSG reductase are given. The set of unitary rate constants for the model described in Fig. 6C that yield the predicted values of these parameters is: $k_1 = 0.85 \times 10^8\ M^{-1}\ s^{-1}$, $k_3 = 10^9\ M^{-1}\ s^{-1}$, $k_8 = k_{10} = 0.50 \times 10^8\ M^{-1}\ s^{-1}$, $k_{12} = 1.0 \times 10^8\ M^{-1}\ s^{-1}$; $k_2 = 0.51 \times 10^3\ s^{-1}$, $k_4 = 7.2 \times 10^3\ s^{-1}$, $k_5 = 0.81 \times 10^3\ s^{-1}$, $k_6 = 1.0 \times 10^3\ s^{-1}$, $k_7 = k_9 = 10^6\ s^{-1}$, $k_{11} = 7.0 \times 10^6\ s^{-1}$

Parameter	Predicted value	Literature value
K_m^{NADPH}	8.52 μM	8.5 μM [63]
K_m^{GSSG}	65.2 μM	65 μM [63]
$K_i^{NADP^+}$	70.0 μM	70 μM [63]
K_i^{GSH}	20[a] mM	'very high'[a] [63]
$K \times [H^+]$	52.5	53 [66]
k_{cat}	724 s^{-1}	724[b] s^{-1}

[a] Inhibition by GSH requires very high (> 6 mM) concentrations of GSH and has not been reliably quantified although it appears to be competitive with GSSG [63]. Derivation of a meaningful expression for K_i^{GSH} is complex so rather than trying to evaluate K_i^{GSH}, we assumed that the dissociation constant for each GSH molecule was 20 mM.

[b] Derived in text.

mass 100000 [65] and, thus, $k_{cat} = 724\ s^{-1}$. From the erythrocyte GSSG reductase activity of 2940 μmol min^{-1} (l cell water)$^{-1}$ (Table 1) we can calculate an active enzyme concentration of 125 nmol (l cell water)$^{-1}$. The actual total GSSG reductase concentration is higher than this since the enzyme is incompletely saturated with the prosthetic group FAD in human erythrocytes [63].

The equilibrium constant of the reaction,

$$K = \frac{[NADP^+][GSH]^2}{[NADPH][GSSG][H^+]},$$

has a value of 1.06×10^9 determined at pH 6.8, $I = 0.33$ M, 40°C [66]. This corresponds to a value of $K \times [H^+]$ of 53 M at pH 7.3.

Gluconolactone-6-P hydrolysis

The primary product of the G6PD reaction is the δ-lactone of gluconate-6-*P*, which is unstable in aqueous solution [67]. Estimates of $t_{1/2}$ for spontaneous hydrolysis of the δ-lactone include 1.5 min at pH 7.4 (temperature not stated but presumably ≈ 25°C) [34], 7 min at pH 7.0, 25°C [67] and 16.2 min at pH 7.4, 34°C [33]. The 6-phosphogluconolactonase has only recently been purified from (bovine) erythrocytes. Kinetic parameters of this enzyme were calculated from data obtained using the more stable synthetic substrate, γ-gluconolactone-6-*P*. The enzyme was purified (3700-fold) to apparent homogeneity and a specific activity of 28.6 μmol min^{-1} mg^{-1}, a turnover number of 14.3 s^{-1} and a K_m value of 0.83 mM were determined for the γ-lactone at pH 7.4, $I = 0.05$ M, 25°C [33]. These authors reported that the human erythrocyte 6-phosphogluconolactonase activity was 14.5 μmol min^{-1} (g wet tissue)$^{-1}$ when assayed with the γ-lactone; this was 6.20 times their measured G6PD activity (assay conditions not specified). They also stated that the K_m for the natural (δ) substrate was of the same order of magnitude as that reported for the rat liver enzyme (80 μM) [67] but neglected to mention the values. 6-Phosphogluconolactonase was incorporated into the simulation scheme as follows.

We assumed that the turnover number, and thus the specific activity, of the bovine erythrocyte enzyme was the same for the δ-lactone as for the γ-lactone and that these values also applied to the human erythrocyte enzyme; this seemed reasonable despite the difference in affinity for the two lactones. The value of k_{cat} was corrected for 37°C by dividing the activity at 25°C by 0.5, which is in the range reported by Beutler [21] for other erythrocyte enzymes. It was also assumed that the activity of 6-phosphogluconolactonase with δ-gluconolactone-6-*P* in human red cells was 6.20 times the

Table 8. *Kinetic parameters used in the 6-phosphogluconolactonase model*
The reported values for some steady-state kinetic parameters of bovine erythrocyte 6-phosphogluconolactonase are given. The set of unitary rate constants for the model described in Fig. 6D that yield the predicted values of these paramters is: $k_1 = 1.3 \times 10^7\ M^{-1}\ s^{-1}$; $k_2 = 1000\ s^{-1}$, $k_3 = 29\ s^{-1}$

Parameter	Predicted value	Literature value
$K_m^{\gamma\text{-gluconolactone-6-}P}$	–	0.83 mM [33]
$K_m^{\delta\text{-gluconolactone-6-}P}$	80 μM	80[a] μM [33]
k_{cat}	29 s^{-1}	29[b] s^{-1}

[a] Assumed value, see text.
[b] Calculated for the human erythrocyte enzyme, see text.

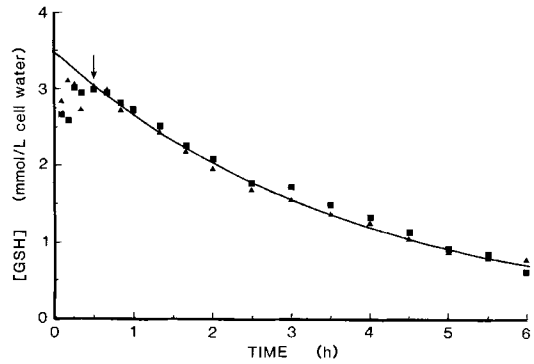

Fig. 7. *Oxidation of GSH in glucose-free human erythrocytes at 37°C.* Freshly drawn venous blood was washed at room temperature twice in 0.9% (w/v) NaCl and twice in Krebs bicarbonate buffer. The cell suspension (haematocrit = 0.60) was then incubated at 37 C under an humidified stream of gas (O_2:CO_2 = 19:1) and GSH was assayed chemically. The data are from two parallel experiments. The solid line is the weighted mean of non-linear regression of a single exponential function onto each data set commencing at the arrow

Table 9. *Concentrations of metabolites used in the computer simulations*
Values from the literature for normal erythrocytes are given. The initial concentrations used in the computer simulations were those expected in glucose-free erythrocytes which had been treated with *t*-butyl hydroperoxide, as described in Methods

Metabolite	Initial concentration in computer simulations	Concentration in normal erythrocytes
	mmol (l cell water)$^{-1}$	
GSH	0.01	3.20 [21]
GSSG	1.60	0.06 [21]
NADPH	0.001	0.0643 [7]
$NADP^+$	0.065	0.0014 [7]
MgATP	1.44[a]	1.44 [24]
MgADP	0.31[a]	0.31[b] [21]
Glycerate-2,3-P_2	3.2	3.2 [24]
Glucose-1,6-P_2	0.11	0.11 [31]
CO_2 (dissolved)	1.2	1.2 [68]
Glucose-6-*P*	0.001	0.040 [21]
Gluconolactone-6-*P*	1×10^{-7}	–[c]
Gluconate-6-*P*	0.0001	–[c]
Ribulose-5-*P*	0.0001	–[c]
Glucose	10.0	5.0

[a] Concentration held constant during simulation.
[b] Assuming that all ADP is Mg^{2+}-bound.
[c] Values not known.

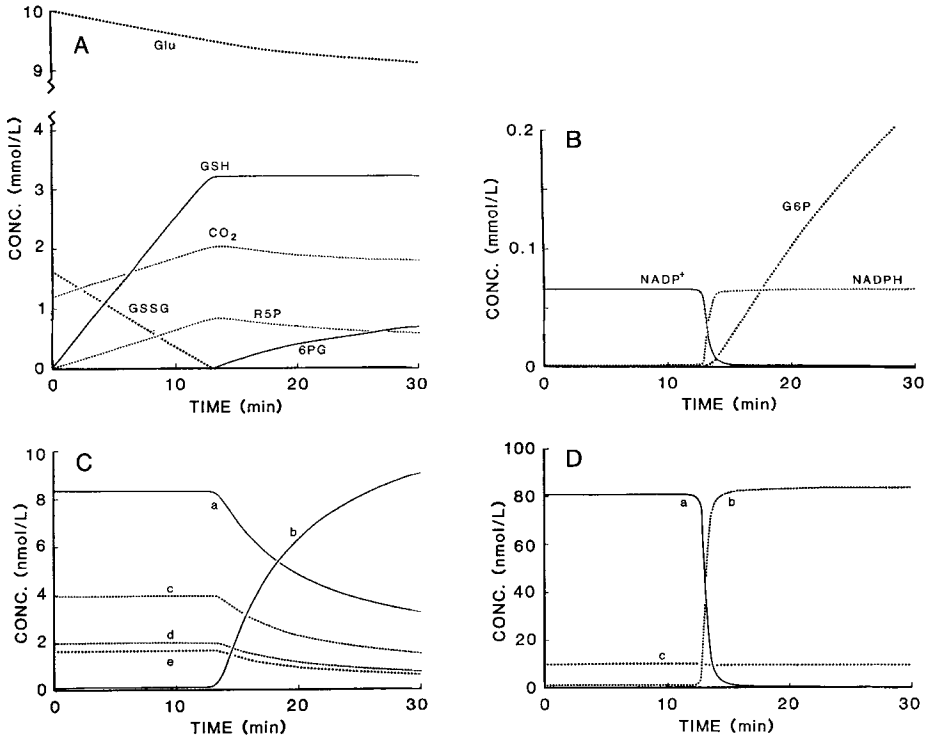

Fig. 8. *Computer-simulation time courses of metabolites and some enzyme species in the model describing glucose-free erythrocytes treated with t-butyl hydroperoxide and supplied with glucose at 0 min.* The calculated time courses of the following compounds are shown: (A) glucose (Glu), GSH, GSSG, CO_2, ribulose-5-*P* (R5P), gluconate-6-*P* (6PG); (B) glucose-6-*P* (G6P), $NADP^+$ and NADPH. The computed concentrations of the following metabolites remained approximately constant and only those varying from $t - 0$ to $t - 30$ min are shown: MgATP (1.44 mM), MgADP (0.31 mM), free glycerate-2,3-P_2 (3.2 mM), glucose-1,6-P_2 (0.11 mM) and gluconolactone-6-*P* (≈ 0.1 μM). The simulated time courses of the predominant enzyme species of (C) HK and (D) G6PD are also shown. The major HK species were (C) a, enzyme – glucose – glucose-1,6-P_2; b, enzyme – glucose – glucose-6-*P*; c, enzyme – glucose; d, enzyme – glucose – glycerate-2,3-P_2 and e, enzyme – glucose – MgATP. The seven other enzyme species in the HK model accounted for less than 7% of the total enzyme concentration during the simulation. The major G6PD species were (D) a, enzyme – $NADP^+$; b, enzyme – NADPH and c, free enzyme. The two other enzyme species in the G6PD model accounted for less than 2% of the total enzyme concentration during the simulated time course

G6PD activity measured by us (Table 1), i.e. 24000 μmol min^{-1} (l cell water)$^{-1}$. Given that the active form of the bovine erythrocyte enzyme is a monomer of relative molecular mass 30000 [33], we calculated an enzyme concentration of 14.0 μmol (l cell water)$^{-1}$.

Since the reaction would be essentially irreversible in aqueous solution the enzyme was assumed to operate by a simple unireactant mechanism as shown in Fig. 6D and the steady-state rate equation was, thus:

$$\frac{d[P]}{dt} = \frac{k_{cat}[A][E_t]}{K_m + [A]} \quad (4)$$

where $k_{cat} = k_3$, $K_m = (k_2 + k_3)/k_1$ and the symbols relate to the annotation used in Fig. 6D. The values of the kinetic parameters used are given in Table 8. Unless otherwise specified, the rate constant for spontaneous hydrolysis of δ-gluconolactone-6-*P* used in the simulations was that obtained from the most recent work (7.1×10^{-4} s^{-1}, pH 7.4, 34 °C) [33].

'Spontaneous' oxidation of GSH

GSH is continually oxidised, by various spontaneous and enzyme-catalysed reactions, during erythrocyte metabolism. Normally the rate of production of reducing equivalents balances the oxidation so that the GSH concentration is maintained at a steady level. In the absence of a source of reducing equivalents, the GSH level will fall as oxidation continues. This continuous oxidation of GSH was studied and the results were incorporated into the simulation scheme as follows.

Glucose-free human erythrocytes were prepared as described in Methods. Duplicate preparations were incubated at 37 °C and periodically sampled for GSH determination; the results are shown in Fig. 7. The GSH concentration remained roughly constant for about 30 min after the start of the incubation, presumably until all intermediates from which NADPH could be produced were exhausted. A single exponential function was fitted to each data set, commencing at 30 min. The data were well described by this function and a value of $t_{1/2} = 157 \pm 3$ min (weighted mean ± grouped standard deviation, $n = 2$) was calculated. A unimolecular rate constant, $k = 7.4 \times 10^{-5}$ s^{-1}, was thus incorporated into the simulations to describe the reaction GSH → 0.5 GSSG.

In 'unstressed' erythrocytes, with a GSH concentration of 3.2 mmol (l cell water)$^{-1}$, this corresponds to a continuous oxidation of GSH of 0.80 mmol h^{-1} (l cell water)$^{-1}$. Maintenance of GSH in the reduced state would therefore require a minimum flux of 0.20 mmol h^{-1} (l cell water)$^{-1}$ through the HMS, assuming that the derived rate constant adequately describes GSH oxidation. The normal rate of glucose consumption is 1.4–2.9 mmol h^{-1} (l cell water)$^{-1}$ [1] and the amount of glucose metabolised by the HMS has been estimated to represent 6–11% of this [3, 4, 9]. This corresponds to a measured flux of 0.08–0.32 mmol h^{-1} (l cell water)$^{-1}$ through the HMS which agrees with the value calculated from our estimated rate constant.

Concentrations of metabolites

The starting concentrations of metabolites used in the computer simulations were those given in Table 9, unless otherwise stated. In simulations of GSH production in the reconstituted metabolic systems, the initial metabolite concentrations were those used experimentally in the reconstituted system.

Fig. 8 shows the simulated time courses of the chemical species in the model. GSSG reduction proceeded over about the first 13 min of the simulation (phase 1) and during this time the levels of CO_2 and ribulose-5-*P* increased while glucose fell (Fig. 8A) and gluconate-6-*P* (Fig. 8A), glucose-6-*P* and NADPH (Fig. 8B) remained at low levels. When reduction was nearly complete (start of phase 2) the rate of glucose consumption started to decline, NADPH replaced $NADP^+$ as the predominant form of the coenzyme (Fig. 8B) and glucose-6-*P*

and gluconate-6-*P* accumulated to higher than physiological levels. The excessive accumulation of the hexose and pentose phosphates and the fall in CO_2 and ribulose-5-*P* following GSH regeneration are artefactual, resulting from inadequate description of the system behaviour by the model at high GSH levels and the absence of a sink for ribulose-5-*P*. They occur because the model is of a subsystem rather than of the entire glucose metabolism of the erythrocyte. Although the model is not generally applicable it is suitable for studying the regulation of the HMS under conditions of oxidative stress when the HMS is the predominant pathway of glucose utilisation [2–4, 9].

Simulations of the temporal distribution of the major enzyme species are also shown for HK (Fig. 8C) and G6PD (Fig. 8D). Other simulations of the initial phase of the system predicted that the pseudo-steady-state distributions of the enzyme species (during phase 1) were established within about 0.5 ms from the start of the simulation. All the major HK species (Fig. 8C) were glucose-associated since the glucose concentration was more than 100-fold greater than its K_m value. The most abundant enzyme complex during phase 1 was the enzyme–glucose–glucose-1,6-P_2 form which represented about 50% of the total enzyme concentration. The enzyme–glucose–glucose-6-*P* form remained low during phase 1 due to the low levels of free glucose-6-*P*; the level of the complex increased in phase 2, to become the preponderant species. The extent of this increase, however, was more than would be anticipated for the system *in situ* since the marked accumulation of glucose-6-*P* in the simulation (Fig. 8B) does not occur *in situ*. At the normal physiological value of glucose-6-*P* (Table 9) the latter enzyme form represents 22% of the total while the enzyme–glucose–glucose-1,6-P_2 form represents 39% of the total. This comparison shows the relative importance of glucose-1,6-P_2, compared to glucose-6-*P*, as a regulator of HK activity under normal conditions; it also illustrates the limitation it exerts on the rate of generation of reducing equivalents under conditions of oxidative stress. The influence of free glucose-1,6-P_2 on HK at physiological concentrations of P_i and Mg^{2+} is likely to be even more important relative to that of glucose-6-*P*.

The most abundant G6PD form during phase 1 of the simulation (Fig. 8D) was the binary $NADP^+$ complex, but this was superseded by the binary NADPH complex in phase 2, thus mirroring the predicted change in the $NADP^+$/NADPH ratio (see Fig. 8B).